Open Medscience

Peer-Reviewed Open Access

JOURNAL OF DIAGNOSTIC IMAGING IN THERAPY

Journal homepage: www.openmedscience.com

Review Article

Bifunctional Metal - Nitroimidazole Complexes for Hypoxia Theranosis in Cancer

Carolynne L. Ricardo, Piyush Kumar*, Leonard I. Wiebe

Department of Oncology, Faculty of Medicine and Dentistry, University of Alberta, Edmonton, Alberta, Canada

*Author to whom correspondence should be addressed:
Piyush Kumar, Ph.D.
Department of Oncologic Imaging, Cross Cancer Institute, 11560 University Avenue, Edmonton, Alberta, Canada T6G 1Z2. E-mail: pkumar@ualberta.ca

Abstract

Oxygen supply - demand imbalances can render proliferating cells acutely or chronically hypoxic. In cancer cells, hypoxia-induced pathophysiological changes give rise to genetic changes that lead to treatment-resistant, aggressive phenotypes. The reduced curability of hypoxic tumours by radiotherapy is one of consequent challenges, but their hypoxia also offers unique, exploitable properties. Nitroimidazoles, for example, capitalize on oxygen-sensitive reductive activation to achieve hypoxia-selective localization for theranostic consequence. The discovery of 2-nitroimidazole (azomycin) heralded the development of many drugs, including effective radiosensitizers of hypoxic cells. These electron-affinic, reductively bioactivated nitroheterocyclics undergo initial oxygen-reversible, enzymatic one-electron reductions that lead to the formation of molecular adducts that impair vital

ISSN: 2057-3782 (Online)
http://dx.doi.org/10.17229/jdit.2015-0415-015

molecular processes. Accumulation of radiolabelled adducts within hypoxic cells creates localized, imageable signals and/or radiotherapeutic (MRT) concentrations of the radiopharmaceutical.

The theranostic potential of hypoxia-targeted organometalic nitroimidazole derivatives is imparted by the radioisotope of the selected metal - main group metals (Al, Ga, In, Zn), transition metals (Cu, Tc, Re, Zn) or lanthanides (Gd, Lu). Of these, the transition element complexes of Cu and Tc have received the most attention. Selected ligands comprise a broad range of mono- or poly-dentate, linear or cyclic chelators, which have been modified with hypoxia-selective nitroimidazoles or nitrotriazoles tethered by a variety of linker moieties.

These metal-nitroimidazole complexes have one or more reducible centres (i.e., nitroimidazole; transition metal core), each of which has characteristic redox properties and consequently, unique interactions inside target (hypoxic) and normoxic tissues. In theory, complexes with reducible metal cores (i.e., transition metals) and reducible targeting vectors (i.e., nitroimidazole) potentially offer greater selectivity and sensitivity for hypoxic tissues than either reducible metal-complexes alone or the nitroimidazole without the reducible metal centre.

The current review focuses on the design, radiolabelling chemistry and hypoxia-selective properties of those organometallic complexes that include nitroimidazoles as their bioactive targeting moiety.

Abbreviations: **HSF** (hypoxia specific factor), the ratio of compound uptake by hypoxic cells *vs* uptake by normoxic cells in cell culture; **%ID/g**, concentration of radioactivity expressed as the percent of injected dose per g of tissue; **MN**, metronidazole; **NI**, nitroimidazole; **p.i.**, post injection; **SER(P)**, single-electron reduction (potential); **T/B** and **T/M**, ratio of radioactivity concentrations between tumour and blood, and tumour and muscle, respectively.

Keywords: hypoxia, metal-nitroimidazole complexes, oxygen mimetics, bioreductive activation, molecular adducts, hypoxia-selective theranosis (**Thera**py+diag**nosis**)

1. Reductively bioactivated, oxygen mimetic, hypoxia-targeted radiosensitizers and theranostics

Imbalances between oxygen supply and demand in proliferating cells can render them acutely or chronically hypoxic [1]. Hypoxia has more recently been acknowledged as a hallmark of many pathologies but has been of special interest in cancer for at least five decades. During this time, it has been shown that in oncological disease, hypoxia-induced pathophysiological changes give rise to genetic changes that lead to more aggressive phenotypes with increased metastatic potential, malignant progression and angiogenesis [2-5]. Furthermore, hypoxia complicates prognosis because the low levels

ISSN: 2057-3782 (Online)
http://dx.doi.org/10.17229/jdit.2015-0415-015

of oxygen render biological systems more resistant to the cytotoxic effects of x-rays and gamma-rays, thereby limiting the curability of hypoxic tumours by radiotherapy [6-7].

Hypoxic cancer cells are also resistant to chemotherapy due to their abnormal blood vasculature, which reduces anticancer drug diffusion into tumour cells [7-8]. New strategies for developing hypoxia-selective, efficacious diagnostic and anticancer drugs are therefore a continuing challenge. The discovery of 2-nitroimidazole (azomycin; Figure 1) [9] led to the development of many synthetic nitroimidazole analogues [10-11] that are effective against bacteria and protozoa that thrive under anaerobic conditions.

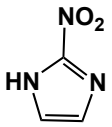

Figure 1. 2-Nitroimidazole (azomycin); $C_3H_3N_3O_2$; mw 113.075 g/mol.

Azomycin and other electron-affinic, reductively-bioactivated nitroheterocyclics also act as hypoxic tissue radiosensitizers. The nitro (-NO_2) group of these nitroimidazole (NI) containing compounds can undergo enzymatic single-electron reductions (SER) to a radical anion [11], a process that is reversible in the presence of oxygen. These nitroimidazoles are not reductively activated in normoxic tissues, and this minimizes their toxicity to healthy proliferating cells. Under hypoxic conditions, however, they undergo further 1- and 2-electron reductions and rearrangements, forming reactive species that can covalently combine with cellular intermediates to form adducts that impair molecular processes and are only slowly cleared. The nitroso, nitrosamine and some rearrangement intermediates are among the most reactive species, whereas the introduction of a total of six electrons affords the amino analogue, which is not sensitive to further reduction. Molecular free radicals generated by ionizing radiation or by bioreductive processes mimic the action of molecular oxygen, forming adducts with nucleophilic cellular macromolecules, a process that causes radiosensitization and prevents or slows egress of the reductively-activated nitroimidazole.

In this scenario, a gradual accumulation of trapped radiolabelled adducts within hypoxic cells creates a localized, discernible signal and/or radiotherapeutic concentration of the radiopharmaceutical. The basic molecular mechanisms of reductively bioactivated nitroimidazoles for imaging and radiosensitization of hypoxic tumours have been extensively reviewed elsewhere [12-14]. A number of radiohalogenated azomycin derivatives [15], [^{18}F]FMISO [16], [^{18}F]FAZA [17] and [^{123}I]IAZA [18], have been used in clinical PET and SPECT diagnostic imaging, respectively. As radiotheranostic drugs (i.e., those with both diagnostic and therapeutic applications), however, the radiofluorinated compounds like [^{18}F]FMISO and [^{18}F]FAZA have no molecular radiotherapeutic (MRT) potential, and of the radioiodinated analogues, only [^{131}I]IAZA has undergone preliminary investigation of its potential for MRT [19].

ISSN: 2057-3782 (Online)
http://dx.doi.org/10.17229/jdit.2015-0415-015

2. Hypoxia-selective bifunctional organometallic coordination complexes

The radioisotopes of several metals have theranostically useful emission properties. Their complexation with appropriate ligands offers simple ('shake and shoot') labelling procedures. These bioactive complexes are made up of a bifunctional chelator, which is covalently attached to a targeting vector through a linker or spacer, and a coordinately-bound radiometallic nuclide [20], as shown diagrammatically in Figure 2. In order to facilitate complexation, the bifunctional ligand must possess a reactive functionality such as an aromatic isothiocyanate, an activated ester or an amine [21-22]. The coordination moiety is attached to a drug or targeting moiety *via* a linker, usually a hydrocarbon, polyethylene glycol (PEG), triazole or polypeptide chain. This 'appendage' alters the pharmacokinetic properties and biodistribution of the metal-ligand unit by modulating the overall charge and hydrophilicity of the drug [21, 23-25]. Since the diagnostic or therapeutic potential is imparted by the radioactive isotope of a metal, there is need for an efficient labelling procedure that will form a highly stable organometallic product. Ligands should therefore have inherent donor atoms (N, O, S) capable of coordinating with the metal ion [22, 26]. The (radio)chemistry of preferred metals and ligands have been the subject of several excellent reviews [27-31].

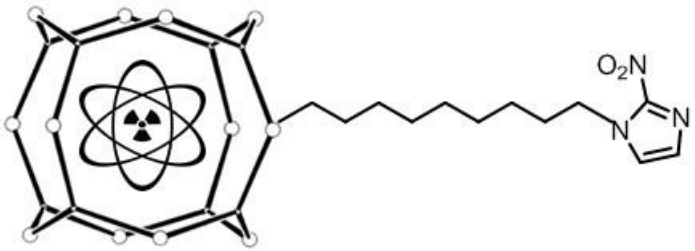

Figure 2. Schematic diagram of a bifunctional nitroimidazole-based radiometallic coordination complex.

The current review focuses on those organometallic complexes that include nitroimidazoles as their bioactive targeting moiety (Figure 2). The reported nitroimidazole derivatives, which have been evaluated for their feasibility as hypoxia markers, include complexes of main group elements (Al, Ga, In, Zn), transition metals (Cu, Tc, Re, Zn) and lanthanides (Gd, Lu). Of these, the transition element complexes of Cu and Tc have received the most attention. The ligands span a wide range, from mono- to polydentate and linear to cyclic chelators, and the bioreducible component includes 2-, 4-, or 5-nitroimidazoles, or nitrotriazoles. The metal nitroimidazole complexes may have one or more reducible centres, namely the nitroinidazole, and depending on the redox chemistry of the metal core, the metal itself. In theory, the complexes containing both a reducible metal core and a targeting vector (i.e., nitroimidazole) potentially offer greater selectivity for hypoxic tissues than either the reducible metal-complex alone or the nitroimidazole without the reducible metal centre.

ISSN: 2057-3782 (Online)
http://dx.doi.org/10.17229/jdit.2015-0415-015

However, this is not always the case. In the butyleneamine oxime (BnAO) series (see the section on ^{99m}Tc-complexes), for example, the nitroimidazole-containing member was the less effective of the HL-91 / HL-91-NI pair when evaluated in a murine *in vitro* cardiac perfusion model and *in vivo* in a canine cardiac stenosis models [32].

On the other hand, for one bis(thiosemicarbazonato)Cu(II) / bis(thiosemicarbazonato)Cu(II)-NI pair (see the section on Cu-complexes) the nitroimidazole analogue was more promising [33].

3. Nitroimidazole-based transition metal coordination complexes

3.1. Copper-based nitroimidazole complexes

Copper has two main oxidation states, Cu(I) (Cu^{1+}) and Cu(II) (Cu^{2+}), and a relatively rare Cu(III) (Cu^{3+}) state [34]. Copper(I) has a d^{10} electronic configuration which yields complexes that are labile have low kinetic stability and are prone to oxidation. Copper(II), the more predominant species, is paramagnetic, with a d^9 configuration providing crystal-field stabilization. This property enables the formation of complexes with square planar, trigonal pyramidal or distorted octahedral geometry. The single electron reductions of Cu^{2+} and Cu^{1+} are facile, and hence very useful in the development of agents to assess hypoxia [35]. Complementary to this feature is copper's wide range of potentially useful radionuclides including ^{60}Cu, ^{61}Cu, ^{62}Cu, ^{64}Cu and ^{67}Cu [36]. Among the copper isotopes, ^{64}Cu is the most versatile and well-suited for PET imaging and targeted radiotherapy, owing to its decay *via* electron capture (41%), β^- (40%), β^+ (19%), and an abundance of Auger electron emissions to supplement radiotherapeutic dosimetry. Copper-64 has a relatively long half-life ($t_{1/2}$ 12.7 h) that accommodates the time constraints of both radiopharmaceutical synthesis and the *in vivo* kinetics of its molecular carriers. The radiodosimetries of ^{64}Cu and ^{67}Cu (100% β^- decay) appear to be suitable for effective MRT [36].

3.1.1. Copper bis(thiosemicarbazone) nitroimidazoles

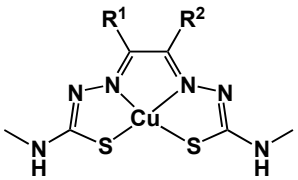

Figure 3. General structure of copper(II)-bis(thiosemicarbazones).

Bis(thiosemicarbazone) ligands (Figure 3) form stable complexes with Cu(II) [35, 37-38]. Several such complexes have been identified as useful agents for the assessment of tumour hypoxia and blood flow [35,38]. Nitroimidazole moieties have been conjugated to diacetyl-bis(N^4-methylthiosemicarbazonato)copper(II) on the premise that the redox trapping mechanisms (i.e., metal

ISSN: 2057-3782 (Online)
http://dx.doi.org/10.17229/jdit.2015-0415-015

reduction and nitroimidazole reduction) could lead to synergistic activity as compared to the individual components. This could result in faster hypoxia uptake or improved sensitivity towards low oxygen concentrations in various hypoxic tumour types. An example includes the nitroimidazole derivative (Cu-H_2ATSM/A-4) (**4**, Figure 4). When compared to ^{64}Cu-ATSM, this compound is relatively more lipophilic due to the presence of the nitroimidazole group. *In vitro* studies showed rapid uptake of this compound by hypoxic cells, reaching a maximum at 5 min and remaining constant for up to 60 min [39].

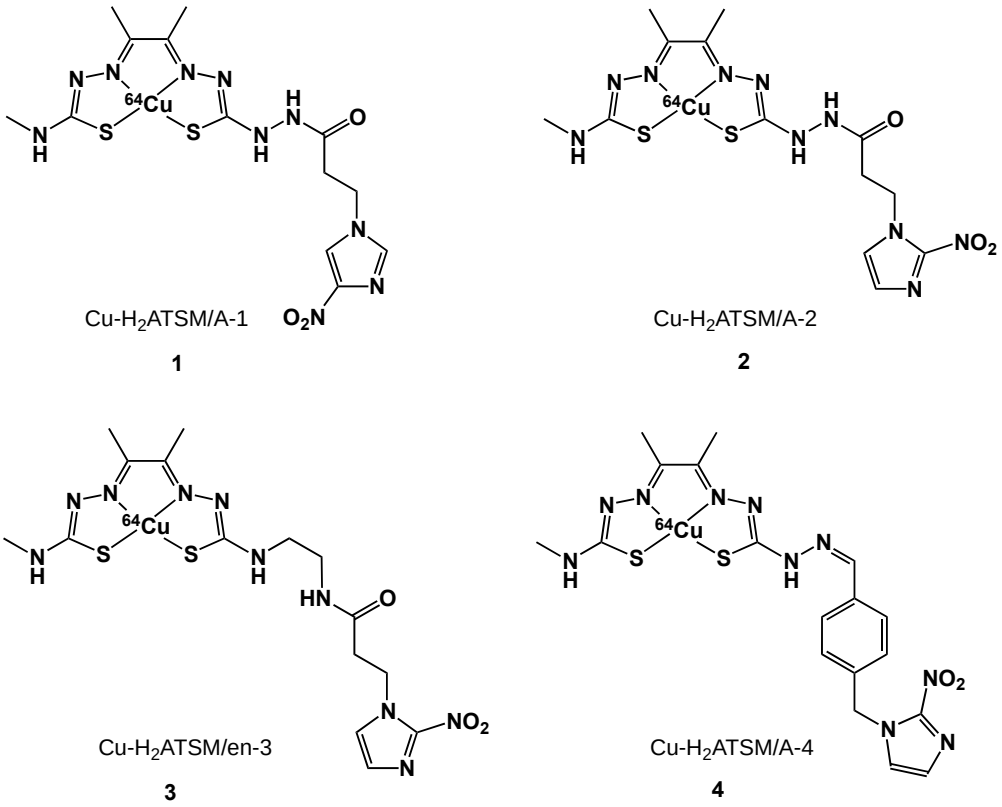

Figure 4. ^{64}Cu-bisthiosemicarbazone nitroimidazoles.

Related compounds include conjugates derived from the diacetyl-bis(N^4-methylthiosemicarbazone) (H_2ASTM/A) platform linked to 2- or 4-nitroimidazole, and diacetyl-2-(4-*N*-methyl-3-thiosemicarbazone)-3-(4-*N*-ethylamino-3-thiosemicarbazone) (H_2ASTM/en; **3**, Figure 4) [33]. Cyclic voltammograms displayed quasi-reversible reduction waves centred at -0.60 V, which was attributed to the reduction of Cu^{II} to Cu^{I}. The most negative reduction potential (-0.63 V) was observed for Cu-H_2ASTM/en-3 (**3**, Figure 4), which was comparable to Cu-ASTM (-0.64 V). Cu-H_2ASTM/A-1 (**1**, Figure 4) and Cu- H_2ASTM/A-2 (**2**, Figure 4) gave values of -0.57 V and -0.58 V, respectively.

In addition to reduction of the metal-centre, the nitroimidazole group displayed quasi-reversible reduction waves attributed to the reduction potentials of 4-nitroimidazole (-1.3 V) and 2-nitroimidazole

ISSN: 2057-3782 (Online)
http://dx.doi.org/10.17229/jdit.2015-0415-015

(-1.0 V). Based on the logarithmic values of the partition coefficients (log*P*), which ranged from 1.13 to 1.45, these compounds were considered to be more hydrophilic than Cu-ASTM (log*P* 1.85). This reduced lipophilicity was attributed to the presence of the amide groups in the linking arms. *In vitro* studies in EMT6 cells showed that the combination of the nitroimidazole and the metal centre resulted in a gradual, hypoxia-sensitive uptake, but with lower final uptake values, compared to the greater and almost instantaneous uptake of the respective non-nitroimidazole Cu complex. Cellular uptake values at 0%, 0.1% and 0.5% of oxygen were 92.6%, 81.9% and 73.5%; respectively.

Among the nitroimidazole-containing tracers, complex **3** (Figure 4) gave the highest hypoxia-selective factor (HSF, the ratio of uptake in hypoxic cells relative to aerobic cells; also referred to as the hypoxia selective index, HSI) of 0.84 and at the same time exhibited uptakes of 67.2, 66.1 and 64.3% at oxygen levels 0%, 0.1 and 0.5%, respectively. The other 2-nitroimidazole-containing complex (**4**) has an HSF of 0.74, with greater and more selective uptake than the 4-nitroimidazole (**1**) counterpart (HSF 0.64) (See Table 1). The promising results obtained from compound **3** were attributed to its reduced lipophilicity, the Cu(I/II) redox potential and the inclusion of a bioreducible nitroimidazole component. The increased hypoxia selectivity of complex **2** compared to **1** was attributed to the presence of the 2-nitroimidazole group, which has a less negative reduction potential than the corresponding 4-nitroimidazole group.

In biodistribution studies conducted in BALB/c mice bearing EMT6 tumours, complexes **2** and **3** showed blood levels (expressed as %ID/g; percent of the injected dose present per gram of tissue) that declined rapidly, from 4.03 and 3.00 %ID/g at 5 min, to 2.74 and 2.18 %ID/g at 60 min, respectively. Similar tumour uptakes were observed for **2** and **3**, with corresponding values of 2.97 %ID/g and 2.56 %ID/g at 60 min post-injection [33]. The tumour/blood (T/B) and tumour/muscle (T/M) ratios at 60 min for complex **2** were 1.08 and 2.14 while those of complex **3** were 1.17 and 1.87, respectively [33].

3.1.2. Copper polyazamacrocycle nitroimidazoles

Efforts have also been directed to the design of copper radiopharmaceuticals based on bifunctional chelators derived from polyazamacrocycles, which exploit the high affinity of Cu(II) for N, O and S donor atoms and include 1,4,7,10-tetraazacyclododecane-1,4,7,10-tetraacetic acid (DOTA), 1,4,7-triazacyclononane-1,4,7-triacetic acid (NOTA), 1,4,8,11-tetraazacyclotetradecane-1,4,8,11-tetraacetic acid (TETA), 1,4,8,11-tetraazacylotetradecane (cyclam) and cross-bridged cyclam. Reasons given for this interest included the stability and kinetic inertness of these macrocyclic complexes [26, 40].

Among the ^{64}Cu-labelled polyazamacrocyclic ligands reported [26, 40] only one type linked with nitroimidazoles, namely azomycin-cyclam conjugates (**5-9**, Figure 5), have been prepared and labelled with ^{64}Cu for the delineation of tumour hypoxia [41]. These ligands were prepared by condensation of 1,4,8,11-tetrazocyclotetradecane (cyclam) with the 1-(2,3-epoxypropyl)-2-nitroimidazole or 1-(3-bromopropyl)-2-nitroimidazole. Radiolabelling was performed by dissolving the corresponding cyclam

ISSN: 2057-3782 (Online)
http://dx.doi.org/10.17229/jdit.2015-0415-015

derivative and $^{64}CuCl_2$ in distilled water at pH 6.0-7.0, followed by heating the resulting solution to yield **5 - 9**. $CuCl_2$ was added as carrier to improve the radiochemical yield and purity of the final products. Compounds **5** and **6** have corresponding log*P* values of -3.0 and -2.52, lower than those of **7**, **8** and **9** (-1.3, -0.19 and -2.0; respectively), presumably due to the presence of the hydroxyl groups in the linking chain. The *in vitro* uptake and binding of these novel compounds and ^{64}Cu-ATSM were studied using DU-145 prostate tumour cells.

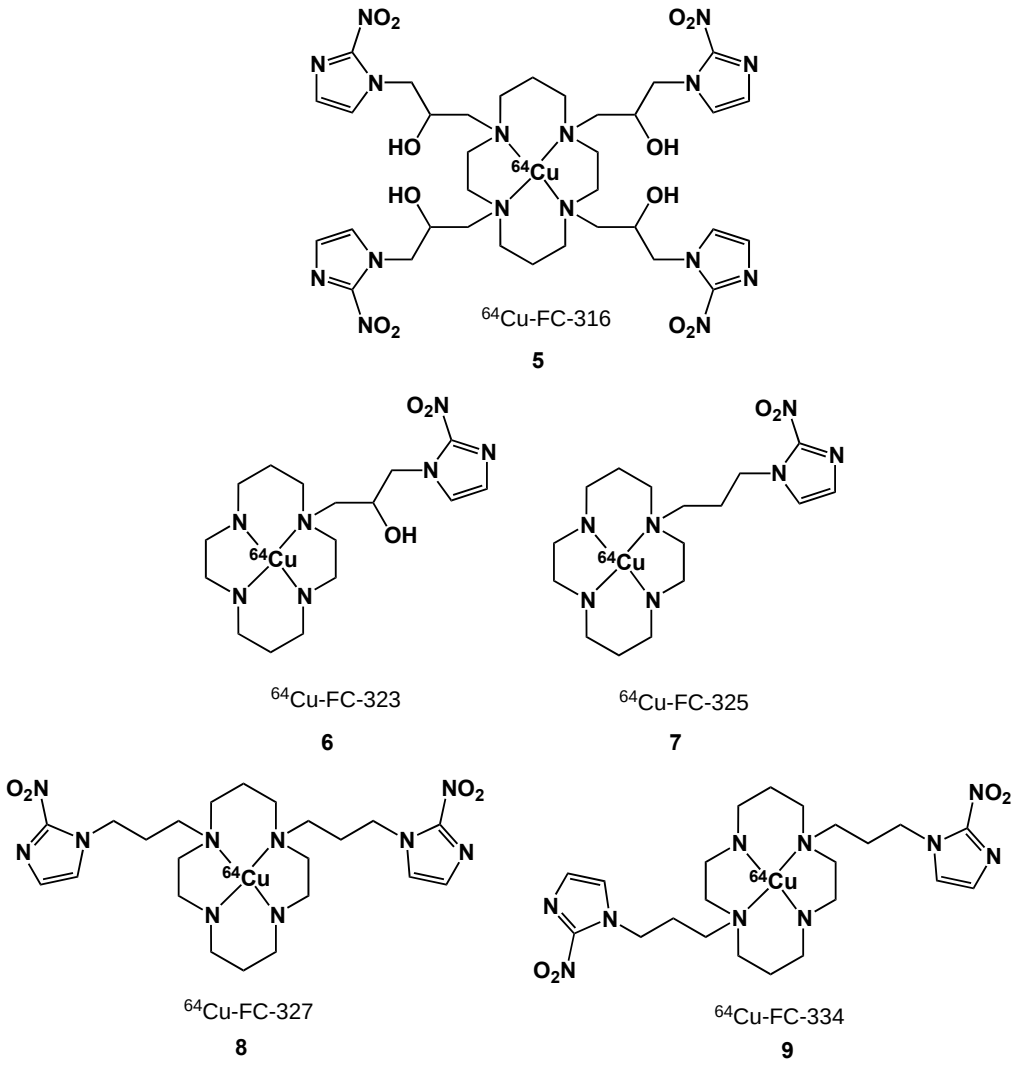

Figure 5. ^{64}Cu-cyclam nitroimidazole complexes.

ISSN: 2057-3782 (Online)
http://dx.doi.org/10.17229/jdit.2015-0415-015

The HSF values for the di-azomycin derivatives (**8, 9**) were ~7, while the HSF's of **5**, **6**, **7** and ^{64}Cu-ATSM were in the 3 – 5 range. Extensive studies of hypoxia marker avidity were performed in rat prostate R3327-AT and R3327-H carcinomas growing in Fisher X Copenhagen rats. ^{64}Cu-ATSM and **5** were retained more in R3327-AT tumours, and the T/B and T/M ratios at 5-6 h post-injection were ~2-3 times higher than in R3327-H tumours.

The respective T/B and T/M ratios for **8** (3.3 and 20.1) and **9** (2.2, 13.6) were higher than those of **5** (1.6, 12.3) and **7** (1.5, 8.9) ^{64}Cu-ATSM (2.1, 10.9) and ^{123}I-IAZGP (3.4, 6.0) in animals bearing R3327-AT tumours. Planar images obtained using **5** showed highest tumour radioactivity relative to non-target organs (gastrointestinal and liver) when compared to other planar/SPECT markers (^{99m}Tc-HL-91, ^{99m}Tc-FC-325 and ^{123}I-IAZGP), indicating that azomycin-cyclam based markers labelled with ^{64}Cu and ^{67}Cu could be used to image tumour hypoxia with PET and SPECT, respectively.

3.2. Rhenium nitroimidazole compounds

In nature, rhenium has one stable isotope (^{185}Re, 37%), one very long-lived radioactive isotope (^{187}Re; $t_{1/2}$ >10^{10} y) and two radioisotopes (^{186}Re, $t_{1/2}$ 90 h; ^{188}Re $t_{1/2}$ 17 h) that have therapeutic and imaging emissions and are therefore of medical interest. Rhenium has five common oxidation states (-1, 2, 4, 6, 7), but also exists in 0 and +1 states. Interest in bifunctional Re complexes relates to the MRT potentials of ^{186}Re and ^{188}Re, and to the molecular modelling and crystallographic properties of stable Re compounds as models for analogous Tc-complexes that are often difficult to determine given the short half-life of ^{99m}Tc and the non-existence of stable Tc isotopes [28]. Re and Tc complexes with the same ligand have essentially the same coordination parameters since the ionic radii of both metals are about the same due to the 'lanthanide contraction' effect. However, their chemistries do differ, for example, the higher oxidation states of Re are more stable and therefore reduced Re radiopharmaceuticals display a greater tendency to undergo re-oxidation to perrhenate [42].

5-Nitroimidazole-Re(CO)$_3$ (**10**, Figure 6) is one of only a few Re-nitroimidazole complexes reported [43]. The HPLC profile of the Re analogue matched that of ^{99m}Tc-IDA-NI. Other examples include Re-Ntm-1(**11**) and Re-Ntm-2 (**12**) (Figure 6), which were both prepared *via* ligand substitution on the precursor *fac*-[NEt$_4$]$_2$[Re(CO)$_3$Br$_3$] [44]. HPLC analyses and UV detection of the Re analogues showed main peaks with the same retention time as the corresponding ^{99m}Tc complexes. The structural characterizations of **11** and **12** were also compatible with the proposed structures of the corresponding ^{99m}Tc complexes, confirming the presence of one ligand coordinating to the ^{99m}Tc-tricarbonyl core and one water molecule to complete the octahedral geometry of **11**.

In another study, the proposed structures of ^{99m}Tc-labelled monoamine-monoamide dithiol (MAMA) ligands containing one or two nitroimidazole moieties were characterized by comparing them with analogous ReO-MAMA compounds (**15**, **16**, **17** and **18**, Figure 6) [45].

ISSN: 2057-3782 (Online)
http://dx.doi.org/10.17229/jdit.2015-0415-015

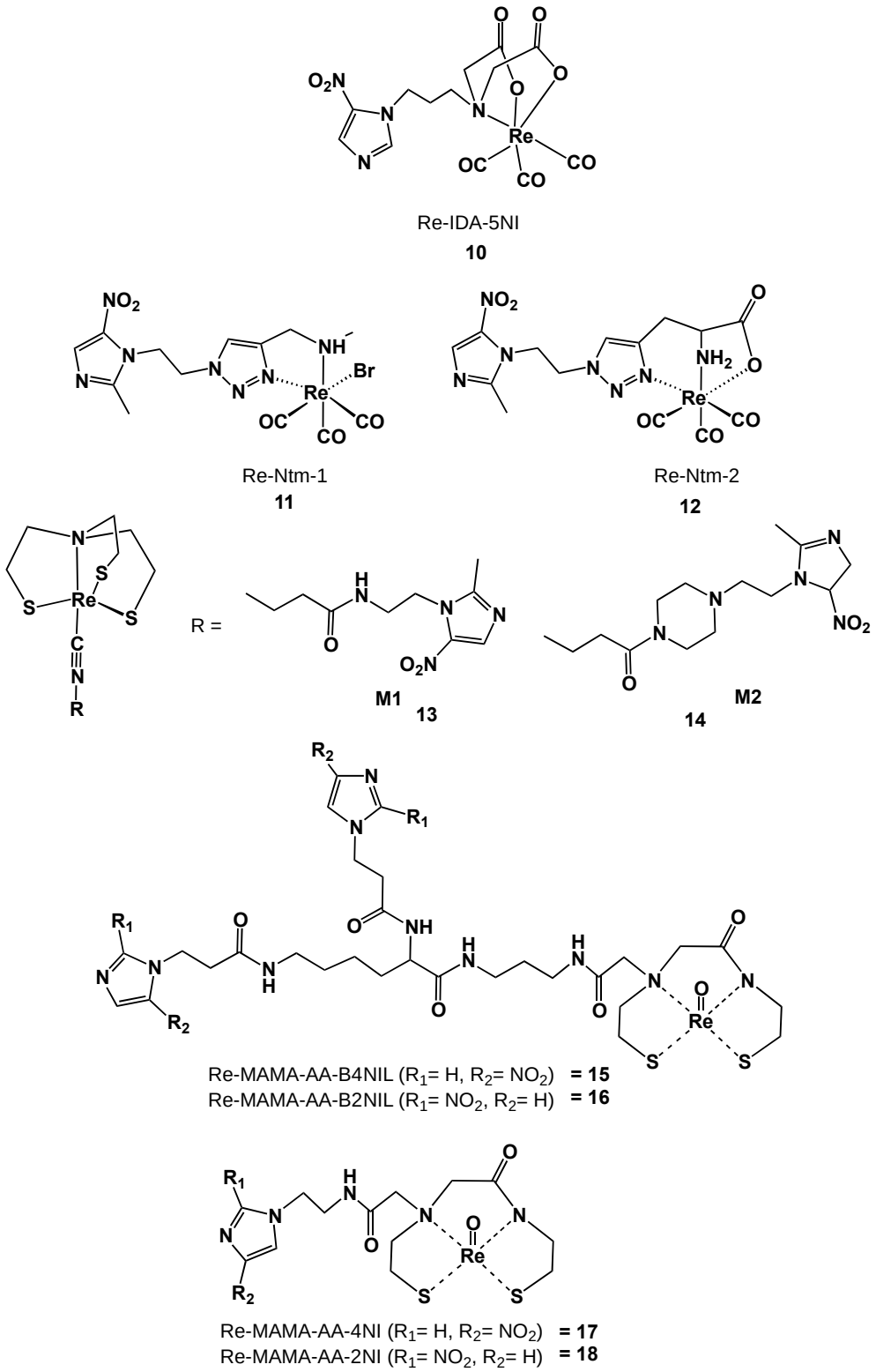

Figure 6. Rhenium nitroimidazole complexes.

ISSN: 2057-3782 (Online)
http://dx.doi.org/10.17229/jdit.2015-0415-015

IR spectra of the resulting complexes displayed the expected [Re=O] stretching band in the region of 950-960 cm^{-1} together with intense bands corresponding to the nitro groups around 1340 and 1500 cm^{-1}. The disappearance of the proton signals corresponding to the trityl groups at 7.20-7.40 ppm in ^{1}H NMR and the change of signals on the MAMA ligands confirmed the formation of ReO-MAMA complexes.

The signals on the skeleton were diastereotopic, indicating that the complexes assumed the square pyramidal configuration. Another characteristic of the ReO-MAMA complexes was the downfield shift of carbon atoms in the ^{13}C NMR spectrum. HPLC analysis for each Re analogue showed one major peak with a retention time similar to that of the corresponding ^{99m}Tc-labelled complex, suggesting identical structures for each of the complexes. In electrochemical studies, the ReO-MAMA complexes displayed 2 or 3 reduction waves, with reduction of the nitro groups occurring between -1.04 and -1.51 V. For the MAMA-mono-nitroimidazole complexes, reduction of the Re(V)-oxo core occurred between -1.84 and -2.01 V. All of the Re complexes showed more negative reduction potentials than the free mono- or bis-nitroimidazole-MAMA ligands (-1.04 to -1.45 V) indicating difficult reduction upon chelation with rhenium metal. Isocyanide-metronidazole derivatives such as 4-isocyano-*N*-[2-(2-methyl-5-nitro-1*H*-imidazol-1-yl)ethyl]butanamide (**13)** and 1-(4-isocyanobutanoyl)-4-[2-(2-methyl-5-nitro-1*H*-imidazol-1-yl)ethyl]piperazine **(14)** (Figure 6) derivatives were synthesized and labelled with ^{99m}Tc to form the corresponding ^{99m}Tc-(4+1) complexes (^{99m}Tc-NS_3-M1 and ^{99m}Tc-NS_3-M2) [46].

In order to corroborate the structure, the rhenium analogues were prepared by ligand substitution of the [$Re(NS_3)(PMe_2Ph)$] precursor (**13, 14)**. HPLC analysis of the reaction mixtures containing the Re-(4+1) complexes displayed similar retention times as those of the corresponding ^{99m}Tc complexes. Elemental microanalyses (C, H, N) of the peaks isolated from HPLC were consistent with the proposed structures. Furthermore, mass spectra indicated the presence of *m/z* fragments corresponding to the expected molecular ions with isotopic distribution of the two rhenium isotopes [46].

3.3. Technetium nitroimidazole complexes

Technetium has no stable isotopes, but more than 35 radioisotopes; of these, ^{99m}Tc has become the workhorse of diagnostic nuclear medicine imaging. The development of ^{99m}Tc radiopharmaceuticals continues because of its affordability, good availability, ideal half-life ($t_{1/2}$ 6 h) and ideal gamma emission energy (143 keV) properties which make it the most widely used radionuclide in clinical nuclear medicine. This transition element exists in several oxidation states including Tc(VII), Tc(VI), Tc(V), Tc(IV) and Tc(III) [47]. Of particular significance in radiopharmaceutical applications is Tc(VII) in pertechnetate ($^{99m}TcO_4^-$), which gives access to the preparation of stable ^{99m}Tc cores after reduction with Sn(II) or sodium boranocarbonate [48].

The radiometallic cores in ligand chelation most often assume the Tc(V) oxidation state in the case of ^{99m}Tc-oxo ($[^{99m}Tc\text{-}O]^{3+}$), ^{99m}Tc-dioxo ($[^{99m}Tc\text{-}O_2]^{+}$) and ^{99m}Tc-nitrido ($[^{99m}Tc\text{-}N]^{3+}$), or as Tc(I) in Tc-tricarbonyl ($[^{99m}Tc\text{-}(CO)_3]^{+}$). Structures of technetium complexes depend on the properties of the

chelating ligands and can vary from penta-, hexa- to heptacoordinated compounds. Readers interested in the redox and coordination properties of Tc are referred to the reviews by Mazzi [47], and Abram and Alberto [48]. A detailed insight into early work with nitroimidazole-^{99m}Tc complexes is available in the review by Nunn *et al.* [49]. In the current review, the ^{99m}Tc-labelled bifunctional nitroimidazole radiopharmaceuticals are classified based on the ligands that make up the radiometal's coordination sphere.

3.3.1. Propylene amine oxime (PnAO)

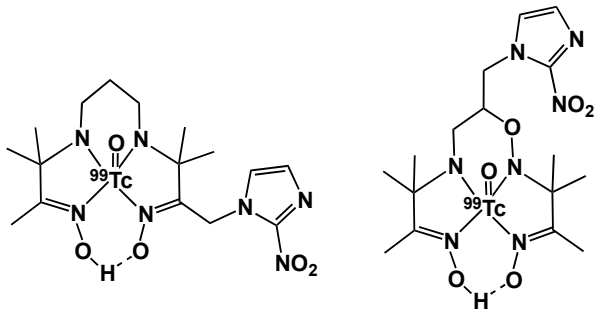

Figure 7. ^{99}Tc-labelled PnAO ligands.

^{99m}TcO(PnAO-1-(2-nitroimidazole) (BMS181321; **19**, Figure 7) is a neutral technetium(V)oxo complex with a 2-NI side-chain linked to the methylene group of the propyleneamine oxime [50]. BMS181321 was the first ^{99m}Tc-labelled 2-NI complex to be widely studied in imaging hypoxia. It is readily prepared at room temperature (~22 ˚C) and pH 8.2, by mixing 3,3,9,9-tetramethyl-1-(2-nitro-1*H*-imidazol-1-yl)-4,8-diazaundecane-2-10-dioxime and sodium pertechnetate ($Na^{99m}TcO_4$) in the presence of stannous tartrate or stannous diethylenetriamine pentaacetic acid (DTPA).

BMS181321 is lipophilic (log*P* ~1.61), rendering it sub-optimal for hypoxia imaging because of its slow clearance from blood and non-target tissues. In order to establish the structure and redox chemistry of BMS181321, a ^{99}Tc standard, ^{99}TcO(PnAO-1-(2-nitroimidazole), was isolated and characterized. X-ray crystallographic analysis demonstrated 4 nitrogen atoms of PnAO coordinating with the Tc(V) centre, with the oxygen atom occupying the apical position resulting in a square pyramidal geometry. Furthermore, the plane of the nitroimidazole group is approximately perpendicular to the plane through the four coordinated nitrogen atoms, and the nitro group is *trans* with respect to the Tc-oxo core. This orientation of the nitroimidazole is very desirable, as it allows access by nitroreductase enzymes. The complex forms a pair of enantiomers, which was resolved using a chiral HPLC column; however it racemizes quickly in the presence of water.

ISSN: 2057-3782 (Online)
http://dx.doi.org/10.17229/jdit.2015-0415-015

Electrochemical studies revealed that the redox chemistry of the nitroimidazole moiety was maintained upon coordination to Tc, with a reversible reduction process at -1.48 V. Additionally, the cyclic voltammogram showed an irreversible reduction process at -1.99 V, which was assigned to the ^{99}Tc-PnAO core [50]. Biodistribution studies performed in mice implanted with KHT, SCC-VII and RIF-1 tumours provided T/M ratios of 3.94, 3.34 and 3.49; respectively, 6 h after intravenous injection [51].

BRU59-21 (oxo[3,3,9,9-tetramethyl-5-oxa-6-(2-nitrol-1-*H*-imidazol-l-yl)-4,8-diazaundecane-2,l0-dione dioximato(3)-*N*,*N*',*N*'',*N*''']-technetium; **20**, Figure 7) was developed to provide lower lipophilicity and better stability than BMS181321 [52]. Modifications included the substitution of one of the methylene carbons in the propylene bridge by oxygen and moving the point of attachment of the 2-nitroimidazole to the position 6 of the chelator. These features did provide greater stability and lower lipophilicity (log*P* 1.04), and consequently, improved pharmacokinetics. Its *in vitro* uptake patterns in CHO cells were similar to that of BMS181321, but the cellular accumulation under both hypoxic and aerobic conditions was lower owing to its lower lipophilicity. After intravenous injection in mice bearing a KHT-C tumour, BRU59-21 was efficiently distributed in various organs and tissues, with significant washout over time compared to BMS181321. Superior T/B and T/M ratios were also observed as a result of rapid clearance from background tissues (blood and muscle) due to the higher hydrophilicity of the tracer. Like BMS181321, its rapid clearance was attributed to hepatobiliary excretion, which limited its use for imaging tumours in the abdominal region.

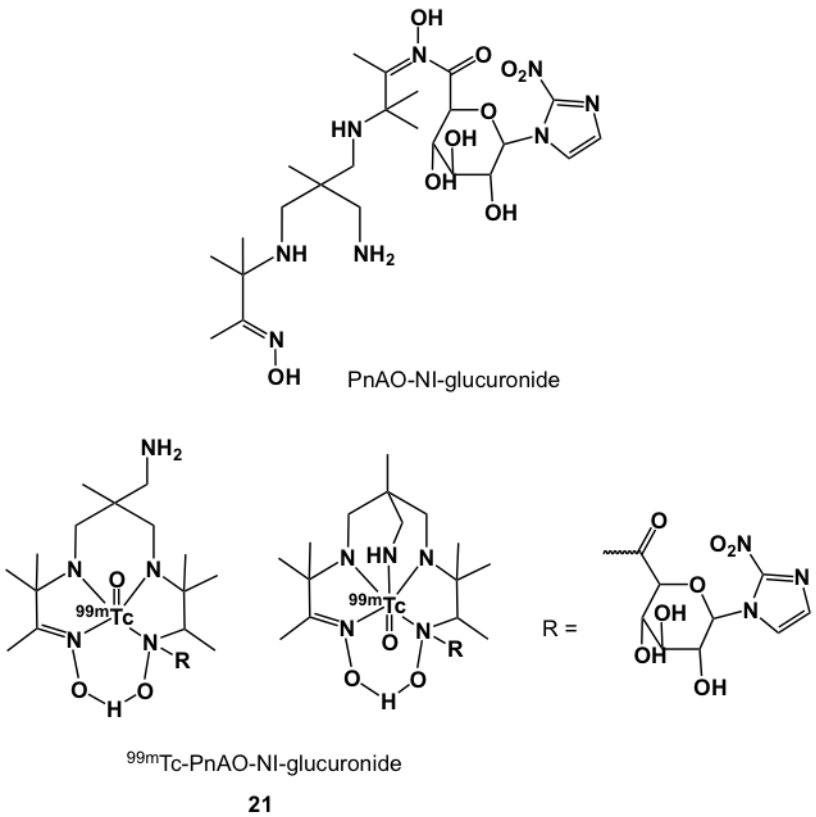

Figure 8. PnAO-nitroimidazole-glucuronide complex, **21**, and the proposed corresponding ^{99m}Tc-labelled conjugates.

ISSN: 2057-3782 (Online)
http://dx.doi.org/10.17229/jdit.2015-0415-015

The azomycin-PnAO conjugate, PnAO-NI-glucuronide (**21**, Figure 8) was synthesized by coupling 1-α-bromo-2,3,4-tri-*O*-acetyl-6-methyl glucuronate to 2-nitroimidazole, followed by deprotection and reaction with 6-methyl-6-methylamino-HMPnAO in the presence of BOP reagent in DMSO to yield the highly water soluble PnAO-NI-glucuronide. Radiolabelling with $^{99m}TcO_4^-$ under reducing conditions produced several ^{99m}Tc-PnAO-NI-glucuronides, in combined 95% radiochemical yield [53]. The structures of two ^{99m}Tc-labelled **21** indicating different Tc-coordination possibilities are proposed (Figure 8). *In vitro* oxygen-dependent binding uptake in EMT-6 cells confirmed their hypoxia avidity but the *in vivo* biodistribution in Balb/c mice bearing EMT-6 tumours was characterized by initial ubiquitous biodistribution of radioactivity, slow non-target organ clearance and hepatobiliary and faecal excretion. At 2 h post-injection, T/B and T/M ratios were 2.5 and 1.0; respectively. The T/B ratio was reported to be comparable to the literature values of IAZA and IAZP and somewhat higher than ^{3}H-MISO and ^{3}H-FMISO [48].

3.3.2. Butyleneamine oxime (BnAO)

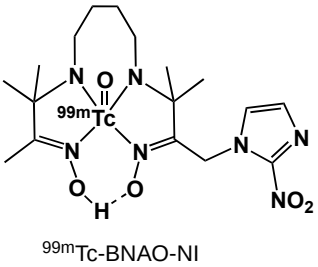

^{99m}Tc-BNAO-NI

22

Figure 9. BnAO-based ^{99m}Tc nitroimidazole complex (HL-91M).

^{99m}Tc-BnAO-NI (**22**, HL-91M; Figure 9) is a 2-nitroimidazole containing analogue of ^{99m}Tc-HL-91 (^{99m}Tc-BnAO) [54]. When compared to the PnAO-based ^{99m}Tc-labelled compounds (**19** and **20**), its accumulation in hypoxic cells was lower, but it exhibited higher hypoxia selectivity as observed with a nine-fold increase in HSF. Evaluation of this complex *in vivo* showed extensive renal clearance and less radioactivity in background tissues. Complex **22** is more lipophilic (log*P* -0.91) than the non-nitroimidazole analogue ^{99m}Tc-BnAO (log*P* -1.05) but more hydrophilic than **19** and **20**. *In vitro* studies in KHT sarcoma cells revealed a 3.57-fold increase in HSF. However, higher specific uptake was observed with the non-nitroimidazole analogue (^{99m}Tc-BnAO) compared to **22**.

In KHT tumour-bearing mice, peak T/B and T/M ratios of 10.32 and 3.96, occurred 2 h after injection. The radiotracer cleared rapidly from the circulation. Small animal SPECT/CT scintigraphic imaging after intravenous injection of radiotracer provided a T/M of 2.59±0.25. Lower radioactive accumulation in tumour (T/M 1.67±0.38) following prior administration pentoxifylline, which has been confirmed to improve oxygenation, reduce tumoural interstitial fluid pressure and delay in tumour growth, was taken as a validation of hypoxia selective uptake [54].

ISSN: 2057-3782 (Online)
http://dx.doi.org/10.17229/jdit.2015-0415-015

The development of **19**, **20** and **22** coincided with an extensive search for 'better' ^{99m}Tc-labelled hypoxia imaging agents by the radiopharmaceutical industry. A summary of BnAO and PnAO related compounds investigated by Amersham International plc, for example, can be found in the manuscript by Archer *et al.* [32].

3.3.3. Boronic acid adducts of technetium dioximes (BATO)

A series of nitroimidazole-BATO (BATO = boronic acid adduct of technetium dioxime) complexes with the general structure $TcX(dioxime)_3BR$ (X = Cl, OH; dioxime = dimethylglyoxime (DMG); R = a nitroimidazole derivative, B = boronic acid) (Figure 10) has been reported [55].

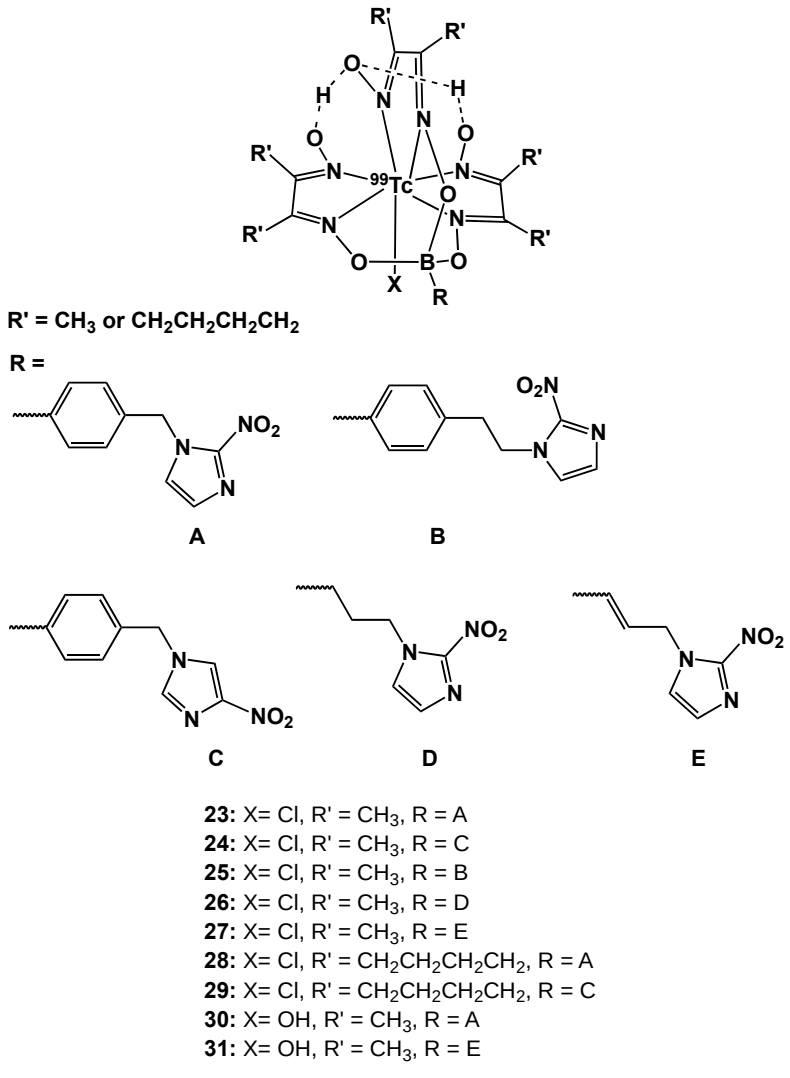

Figure 10. BATO-based ^{99m}Tc complexes.

In these molecules, a 2-nitroimidazole (A, B, D, E) or 4-nitroimidazole (C) moiety was incorporated into the boron cap of the ligand. The BATO-nitroimidazole ligands were directly labelled with either ^{99}Tc(dioxime)$_3$(μ-OH)SnC1 or ^{99}TcCl(dioxime)$_3$ to form complexes **23** to **27**, and ^{99}Tc-cyclohexanedione dioxime (CDO) to afford compounds **28** and **29**. While the preparation of most compounds proceeded in a straightforward manner, TcCl(DMG)$_3$BPhEtNO$_2$ (**25**) was formed from an unidentified intermediate only upon recrystallization from HC1-acidified DMF. Two hydroxy analogues (X = OH, complexes **30**, **31**) were isolated by treatment of the corresponding chloro complexes with aqueous NaOH. Cyclic voltammetry demonstrated the electrochemical reduction potentials of the 2-nitroimidazole-BATO complexes (Table 1) to fall between those of misonidazole and metronidazole, indicating that these compounds could undergo hypoxia-selective binding.

On the other hand, the 4-nitroimidazole counterparts were found to be more difficult to reduce than metronidazole, hence limiting their utility as hypoxia-localizing probes. Enzymatic reduction of the nitro group of the BATO-nitroimidazole complexes by xanthine oxidase was observed but at a slower rate, by at least a factor of 10, when compared to the corresponding nitroimidazole-containing boronic acids. This may, in part, be due to a negative shift in redox potential upon coordination to Tc, or due to the relatively high steric bulk and/or lipophilicity of the technetium BATO complexes. Overall, the data suggest that the BATO-nitroimidazoles may function as hypoxia imaging radiopharmaceuticals [55].

3.3.4. Technetium cyclam nitroimidazoles

N-2'-Methoxyethyl-2-(3'-nitro-1-triazole) acetamide (AK2123; Figure 11) was found to accrue in hypoxic cells and played a role in Phase I clinical trials for the treatment of head and neck cancers [56]. It is less lipophilic than misonidazole and therefore it was expected to have lower neurotoxicity. In order to determine its potential to mark hypoxic regions, this nitrotriazole-based radiosensitizer was conjugated with a macrocyclic ligand, to make cyclam-AK2123 (Figure 11), which was labelled with ^{99m}TcO$_4^-$ using SnCl$_2$-facilitated reduction to provide the complex in over 95% radiochemical purity. ^{99m}Tc-cyclam-AK2123 (complex **32**) was relatively stable up to 3 h, and with its lipophilicity (log*P* -0.10), fell in the optimum range of an ideal hypoxic probe. *In vivo* biodistribution of **32** in normal and mammary-tumour bearing Wistar rats demonstrated selective uptake and accumulation in hypoxic tumours. Biodistribution and scintigraphic imaging on NMU-induced mammary tumour-bearing rats showed a maximal T/M ratio of 8.5 at 5 h post-injection [57].

Due to the good chelating property of cyclam, ^{99m}Tc-labelled complexes of metronidazole derivatives of 1,4,8,11-tetraazacyclotetradecane (cyclam) and 2-oxo-1,5,8,12-tetraazacyclotetradecane (oxocyclam) were developed [58]. Radiolabelling with Na^{99m}TcO$_4$, using stannous tartrate as the reducing agent produced the corresponding complexes in high yields (90-95%) based on chromatographic analysis. The log*P* values obtained for ^{99m}Tc-cyclam-4MN (MN = metronidazole; **33**) and ^{99m}Tc-oxocyclam-4MN (**34**) (Figure 11) were -0.2 and -0.12, respectively, indicating their hydrophilic nature. Uptake of these

complexes in perfused rat hearts showed slightly higher radioactivity retention under normoxic than hypoxic conditions.

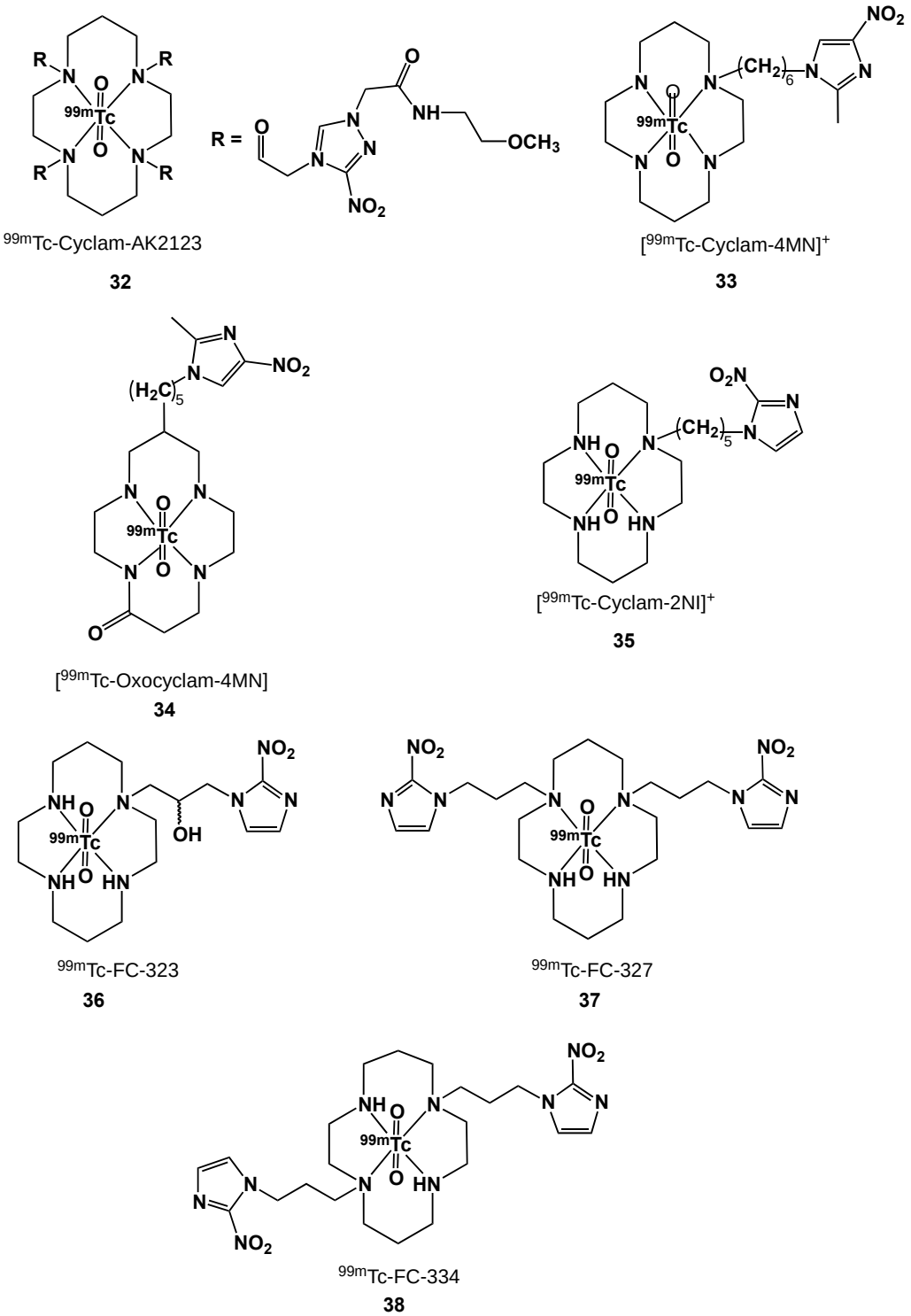

Figure 11. Cyclam-nitroimidazole ^{99m}Tc complexes.

ISSN: 2057-3782 (Online)
http://dx.doi.org/10.17229/jdit.2015-0415-015

The cyclam backbone has also been derivatized with 2-nitroimidazole [59]. Radiosynthesis of ^{99m}Tc-cyclam-2NI (**35**) by the addition of ^{99m}Tc-pertechnetate and $SnCl_2$ afforded high radiochemical yields of a high purity product. *In vitro* assay of ^{99m}Tc-cyclam-2NI in rat mammary tumour and mesothelioma cells showed increasing cell uptake up to 4 h. Biodistribution studies in mammary tumour-bearing rats demonstrated a gradual increase of T/M and T/B count density ratios, with maximum values achieved at 2 h (T/M 5.69; T/B 1.01); rapid clearance from blood and other organs or tissues was observed. Based on the preclinical studies, radiodosimetry calculations for ^{99m}Tc-cyclam-2NI (**35**) indicated that it would be safe to use in humans. Furthermore, scintigraphic images of tumour-bearing rats and rabbits confirmed that tumours could be clearly delineated after the administration of ^{99m}Tc-cyclam-2NI. The T/M ratios at 2 h post-injection in rats and rabbits were 4.2 and 2.98, respectively [59].

Studies of hypoxia marker avidity were conducted using rat prostate R3327-AT and R3327-H carcinoma models. At 5-6 h post-administration to rats bearing the R3327-AT tumour, the T/B and T/M ratios for **36** were 1.9 and 15.8, respectively. These values were significantly higher than the respective values for **37** (0.8, 3.8) and **38 (**1.2, 6.1). Accumulation of **36** was 2-3 times higher in the anaplastic tumour (R337-AT), which is less well perfused than the R3327-H tumour.

3.3.5. Technetium nitroimidazole hydroxyiminoamides

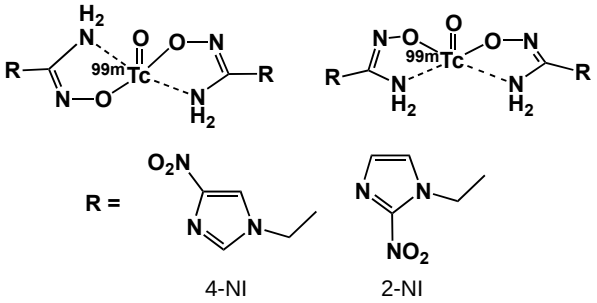

39: R = 2-NI
40: R = 4-NI

Figure 12. ^{99m}Tc-hydroximinoamide complexes.

Hydroximinoamide is a bidentate ligand in which both the N and O atoms act as donor atoms. Nakayama *et al*. reported that chelation of this type of ligand formed ^{99m}Tc complexes that are highly stable *in vitro* and *in vivo* [60-61]. This led to the synthesis of hydroximinoamide derivatives with a bioreducible moiety such as nitroimidazole [62]. In one study, 1-(2-nitroimidazole-1-yl-propan)hydroxyiminoamide was labelled with $^{99m}TcO_4^-$ in the presence of stannous tartrate to obtain the corresponding ^{99m}Tc complex **39** (Figure 12) with radiochemical purity >95%. It is more hydrophilic (log*P* -1.40) than other previously reported hypoxia markers such as BMS181321 (log*P* 1.6), ^{125}IAZA (log*P* 0.46), ^{3}H-misonidazole (log*P* 0.37) and ^{3}H-FMISO (log*P* 0.40). The tissue distribution in mice bearing S180 tumours indicated specific accumulation into hypoxic tumour, with rapid biodistribution and slower clearance from blood during the 2-24 hour period. T/M, T/B, tumour/heart (T/H) and tumour/lung

ISSN: 2057-3782 (Online)
http://dx.doi.org/10.17229/jdit.2015-0415-015

(T/Lu) ratios at 4 h post-injection were 8.4, 1.5, 2.9 and 2.3, respectively. The tumour/liver (T/Li) ratio was 0.6 but increased to 0.9 after 8 h, and 2.3 after 24 h. When compared to other hypoxia-imaging agents, **39** showed T/B values greater than that of BMS181321, but lower than values for ^{125}IAZA, ^{3}H-misonidazole and ^{3}H-FMISO. With the incorporation of 4-nitroimidazole, radiolabelling yields and purity were high, and **40** (Figure 12) was stable *in vitro* and *in vivo* [63].

In S180 tumour-bearing mice, the biodistribution profile of **40** was slightly better than **39**, with T/B, T/M, T/H, T/Lu and T/Li ratios of 1.88, 8.60, 4.47, 2.94 and 0.88, respectively at 4-h post-injection. The optimal values for T/B and T/M, 2.06 and 8.83, respectively, were achieved at 8-h post-injection. Further biological evaluation included *in vitro* assays using CHO tumour cells, biodistribution studies and small animal SPECT imaging of the complex in BALB/c mice subcutaneously injected with U87 (human glioma) or A549 (human lung cancer) cells [64]. High accumulation (40.6% after 4 h) of **40** in CHO cells under hypoxic conditions demonstrated its hypoxia selectivity. At 4 h post-injection, U87-tumour bearing mice had T/B and T/M ratios of 1.98 and 13.11, respectively, and for the A549 cancer cell line, T/M and T/B ratios were 1.25 and 8.48, respectively. SPECT imaging of **40** in both animal models displayed rapid blood clearance, low muscle uptake and relatively high tumour accumulation. Better pharmacokinetics compared to previously reported BMS181321 (**19**) and BRU59-21 (**20**) were attributed to its low lipophilicity (log*P* 0.43).

3.3.6. Technetium nitroimidazole iminodiacetic acids (IDA)

An iminodiacetic acid derivative of metronidazole was obtained by alkylation of 2-methyl-5-nitroimidazole with *N*,*N*-bis[(*tert*-butoxycarbonyl)methyl]-2-bromoethylamine under reflux conditions. Complexation of the bifunctional chelator with $[^{99m}Tc(CO)_3(H_2O)_3]^+$ displaced the 3 H_2O molecules and the vacant sites were coordinated with the N and 2 O atoms, giving **41** (Figure 13) an overall -1 charge [65]. The radiolabelled product was obtained in 96% yield. Biodistribution studies on Swiss mice bearing fibrosarcoma tumours showed uptake of complex **41** with a T/M of 17 at 3 h after injection. The corresponding IDA conjugated to 5-nitroimidazole was also synthesized, radiolabelled and biologically evaluated [43]. This bifunctional ligand was actually obtained as a side-product during the preparation of the 4-nitroimidazole derivative.

The radiolabelled complex **42** was obtained in more than 95% yield. It has higher lipophilicity (log*P* 0.39) than the methyl-substituted 5-nitroimidazole (log*P* -0.82) and demonstrated uptake and slow clearance of radioactivity from tumour in fibrosarcoma bearing Swiss mice. The T/B remained below 1 throughout the 3 h period.

In addition to 5-nitroimidazole substituted IDA (**42**), other derivatives with 2-, and 4-nitroimidazole were synthesized and radiolabeled with $[^{99m}Tc(CO)_3(H_2O)_3]^+$ to form complexes **43** and **44** (Figure 13) in over 95% radiochemical yield [66]. *In vivo* biological evaluations of **43** in Swiss mice implanted with HSDM1C1 murine fibrosarcoma cells as solid tumour models showed higher uptake in hypoxic cells

ISSN: 2057-3782 (Online)
http://dx.doi.org/10.17229/jdit.2015-0415-015

than either **44** or **42** at 30 min post-injection. Clearance from tumour after 60 min was slow for all complexes; however, the relatively slower clearance of **43** was interpreted as indicative of trapping within hypoxic cells. Tumour uptake and retention were correlated with the single electron reduction potential (SERP) of the bioreductively-activated radioactive tracers and their average residence time inside the cell. Complex **43,** with a higher residence time and more positive SERP, showed the highest uptake, followed by complexes **44** and **42**. However, the higher tumour uptake of ^{18}F-FMISO than of **43** was attributed to its higher SERP and longer residence time [67]. The blood clearance pattern was found to be strongly associated with the derived log*P* values of the complexes.

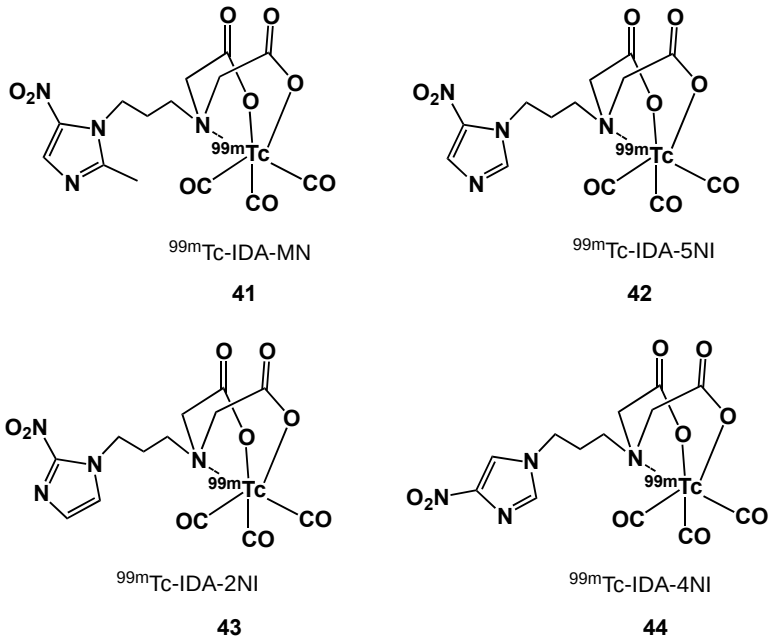

Figure 13. ^{99m}Tc-iminodiacetic acid complexes.

The 2-nitroimidazole complex **43** (log*P* 0.48) cleared relatively slowly compared to **44** (log*P* 0.43) and **42** (log*P* 0.39) [67]. The T/B ratios of **43** and **42** improved with time, reaching maxima of 0.61 and 0.49, respectively, at 3 h post-injection. Radioactivity cleared primarily through the hepatobiliary route for all the three complexes.

3.3.7. Technetium nitroimidazole diethylenetriamines (DETA)

Diethylenetriamine (DETA) is an acyclic amine-based ligand with 3 N donor atoms. Its utility as a bifunctional chelator was explored by conjugating it with a series of nitroimidazole compounds (**45-47**; Figure 14) through a short alkyl chain and subsequent labelling with $[^{99m}Tc(CO)_3(H_2O)_3]^+$ precursor [67]. Substitution of the labile water molecules resulted in the formation of complexes having an overall positive charge with a pseudo-octahedral geometry in which the metal centre is coordinated by three CO ligands and the tridentate DETA through the N atoms.

ISSN: 2057-3782 (Online)
http://dx.doi.org/10.17229/jdit.2015-0415-015

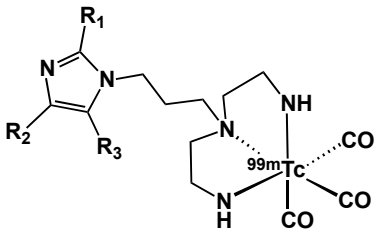

45: ^{99m}Tc-DETA-2NI (R_1= NO_2, R_2= H, R_3= H)
46: ^{99m}Tc-DETA-4NI (R_1= H, R_2= NO_2, R_3= H)
47: ^{99m}Tc-DETA-5NI (R_1= H, R_2= H, R_3= NO_2)

Figure 14. ^{99m}Tc complexes of DETA-nitroimidazole.

The ^{99m}Tc-DETA-NI compounds were obtained in high radiochemical yields and purity, both of which ranged from 94 to 95.3%. Physicochemical evaluations revealed that these radiopharmaceuticals were lipophilic with measured log*P* values of 0.28, 0.17 and 0.15 for **45**, **46** and **47**, respectively. Biodistribution studies of these ^{99m}Tc-DETA-NI compounds and ^{18}F-FMISO were carried out in Swiss mice bearing fibrosarcoma tumour. ^{18}F-FMISO showed significant tumour uptake (4.65 %ID/g at 30 min and 3.70 at 60 min), while only low uptake values were observed for **45-47** (1.05-1.10 at 30 min and 0.31-0.35 at 60 min). Low blood activity was observed as a result of faster clearance of these ^{99m}Tc-DETA-NI radiotracers. T/B ratios obtained at 30 min post-injection for **45, 46, 47** and ^{18}F-FMISO were 1.94, 1.72, 1.26 and 1.17, respectively.

3.3.8. Technetium nitroimidazole triazoles

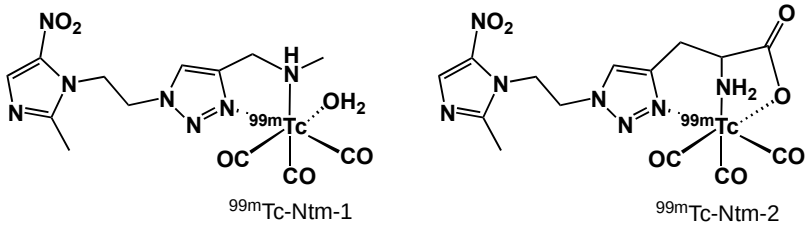

^{99m}Tc-Ntm-1 **48** ^{99m}Tc-Ntm-2 **49**

Figure 15. ^{99m}Tc bi- and tridentate complexes bearing a triazole linker.

Copper-catalysed Huisgen cycloaddition or "click" reaction has been employed in the preparation of suitable bifunctional bidentate and tridentate ligands containing triazole moieties. In particular, **48** and **49** (Figure 15) were designed and synthesized starting with the metronidazole, which was transformed to the corresponding azide *via* the Mitsunobu reaction using azidotrimethylsilane as the nucleophile or converting the -OH group to methylsulfonate followed by a substitution reaction with sodium azide [44]. The organic azide was then reacted with the corresponding alkyne, *N*-methylpropargylamine or propargylglycine using the $CuSO_4$ and ascorbic acid catalytic system to form *N*-methyl-1-[-(2-(2-

ISSN: 2057-3782 (Online)
http://dx.doi.org/10.17229/jdit.2015-0415-015

methyl-5-nitro-1*H*-imidazole-yl)ethyl-1*H*-1,2,3-triazole-4-yl]methylamine (**48**) or 2-amine-3-[1-[2-(2-methyl-5-nitro-1*H*-imidazole-1-yl)ethyl]1*H*-1,2,3-triazole-4-yl]propanoic acid (**49**).

These ligands were labelled with ^{99m}Tc(I)-tricarbonyl precursor to yield the desired complexes in high purity. Complex **48** formed a mixture of two forms, and the ligand was very labile towards displacement by water molecules. On the other hand, complex **49** was stable even 4 h after labelling. Stability in plasma was also higher for **49**, explained by its higher ligand denticity. The relatively low protein binding of Complex **49** was more lipophilic (log*P* -0.44) compared to **48** (log*P* -0.82), but had lower protein binding. Evaluation of these complexes on human colon adenocarcinoma HCT-15 cells demonstrated **49** to have preferential uptake in hypoxic conditions. Biological assessment in C57 mice bearing implanted Lewis lung carcinomas showed that the more stable complex could be a promising hypoxia imaging agent due to the selective uptake and retention in tumour cells, low blood and liver uptake, rapid elimination from blood resulting in high T/B (1.86 at 3 h) and negligible uptake by other organs and tissues.

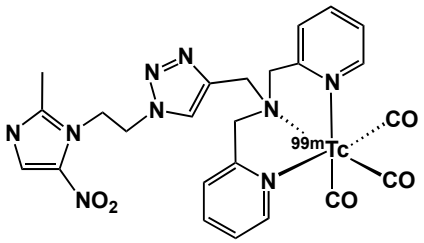

[^{99m}Tc(CO)$_3$(MN-TZ-BPA)]$^+$

50

Figure 16. ^{99m}Tc coordinated to BPA-triazole-metronidazole chelator.

A novel metronidazole derivative [**50**, ^{99m}Tc(CO)$_3$(MN-TZ-BPA)]$^+$; Figure 16) features a 1,2,3-triazole ring which serves as a linker between the bioreductive pharmacophore and bis(pyridine-2-yl)methylamine [68]. This bifunctional chelator has been very attractive for highly efficient introduction of the [^{99m}Tc(CO)$_3$]$^+$ core as a tridentate ligand in the formation of a stable complex. Cu(I)-catalysed coupling of 1-(2-azidoethyl)-2-methyl-5-nitro-1*H*-imidazole and *N*-(pyridine)-2-methyl)prop-2-yn-amine formed the triazole linker, and the second pyridinyl arm was introduced through the addition of 2-(chloromethyl)pyridine to yield *N*-((1-(2-(2-methyl-5-nitro-1*H*-imidazol-1-yl)ethyl-1*H*-1,2,3-triazol-4-yl)methyl)(pyridine-2-yl)-*N*-(pyridine-2-ylmethyl)methanamine.

Radiosynthesis was carried by mixing [^{99m}Tc(CO)$_3$]$^+$ precursor and the tridentate ligand, forming a cationic complex **50** in 95% yield and 90% purity. The compound was hydrophilic (log*P* -1.44) and stable up to 6 h at room temperature after labelling. Biological assessment using Kunming mice xenografted with H22 liver cancer cells showed initial tumour uptake (0.63 ID%/g after 5 min) but unsatisfactory retention (0.12 ID%/g after 4 h). Rapid clearance resulted in low background at 4 h post-injection with values of 0.04 and 0.17 ID%/g for muscles and blood, respectively. The T/B ratio peaked at 0.84, 3 h post-injection [68].

ISSN: 2057-3782 (Online)
http://dx.doi.org/10.17229/jdit.2015-0415-015

3.3.9. Technetium dithiolate and cysteine-based nitroimidazoles

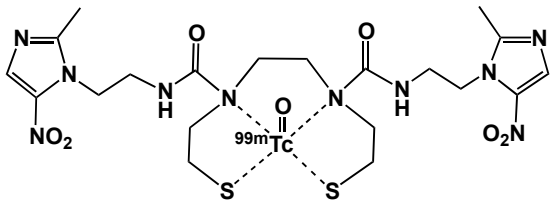

[^{99m}TcO(EC-MN)]$^{+}$

51

Figure 17. Ethylenedicysteine-based ^{99m}Tc complex.

Ethylenedicysteine (EC) is a tetradentate ligand with 2 nitrogen and 2 sulfur donor atoms. Because it forms stable Tc-oxo complexes, its feasibility as hypoxia imaging agent was examined through functionalization of its carboxyl groups with the amino analogue of metronidazole [69]. The synthesis of the conjugate proceeded *via* the transformation of the hydroxyl group of metronidazole to an azido group, followed by reduction with triphenylphosphine. Direct amidation on the carboxylic acid groups of EC in the presence of 1-ethyl-3-(3-dimethylaminopropyl)carbodiimide (EDC) (ethylenediamine hydrochloride) afforded the EC-MN ligand, which when reacted with ^{99m}Tc-pertechnetate under reducing conditions gave **51** (Figure 17) in quantitative radiochemical yield and high purity (95%); it was stable in serum for up to 4 h. In mice inoculated with breast cancer cells, **51** showed a gradual increase in T/B and T/M ratios as a function of time.

The maximum values for T/B (0.66) and T/M (7.14) were obtained at 4 h post-injection. The T/B ratio was not significantly different than for [^{131}I]IMISO at 2 h and 4 h post-injection. Both **51** and [^{131}I]IMISO gave higher T/M ratios than [^{18}F]FMISO. Scintigraphic imaging and autoradiograms of **51** delineated hypoxic tumour [69].

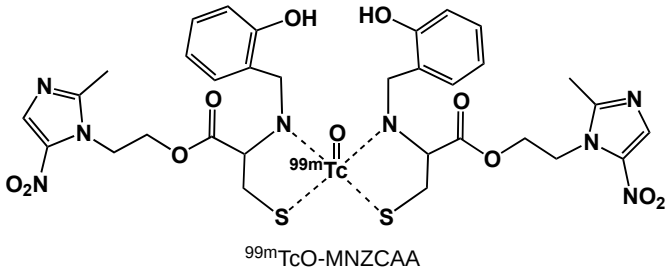

^{99m}TcO-MNZCAA

52

Figure 18. Dithiolate-based ^{99m}Tc complex.

ISSN: 2057-3782 (Online)
http://dx.doi.org/10.17229/jdit.2015-0415-015

The bifunctional chelator *N*-(2'-hydroxybenzyl) cysteine has a free carboxylic acid that was exploited for the introduction of a metronidazole moiety *via* an ester bond [70]. *N*-(2'-Hydroxybenzyl)cysteine was converted to the carboxylic acid chloride and then coupled to the metronidazole tosylate to afford the MNZCAA ligand. Radiolabelling at room temperature was carried out through the $SnCl_2$ or $Sn(C_4H_4O_6)$ mediated reduction of $^{99m}TcO_4^-$ in 85% yield. Complex **52** (Figure 18) was 80% stable for 3 h. Biodistribution in barcl-95 tumour-bearing Swiss mice showed accumulation of radioactivity in tumours and major clearance through the renal and hepatobiliary pathways. T/B ratios increased from 0.43 to 0.82, while T/M ratios increased from 2.98 to 14.67 over the 30 min to 3 h post-injection period, higher than either ^{99m}Tc-BMS181321 (**19**) (2.63) and ^{99m}Tc-BRU59-21 (**20**) (3.63); T/B values for **52** were 0.82, compared to 0.86 for **20** and 0.31 for **19** [70].

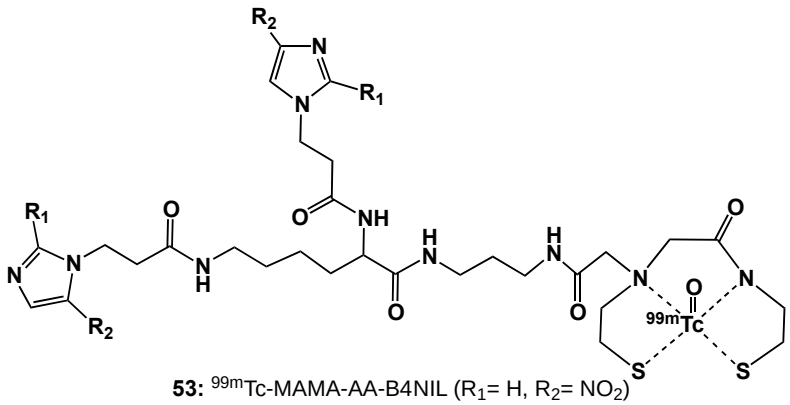

53: ^{99m}Tc-MAMA-AA-B4NIL (R_1= H, R_2= NO_2)
54: ^{99m}Tc-MAMA-AA-B2NIL (R_1= NO_2, R_2= H)

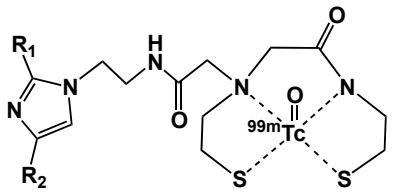

55: ^{99m}Tc-MAMA-AA-4NI (R_1= H, R_2= NO_2)
56: ^{99m}Tc-MAMA-AA-2NI (R_1= NO_2, R_2= H)

Figure 19. Monoamine-monoamide dithiol ligands complexed with ^{99m}Tc-oxo core.

Monoamine-monoamide dithiol (MAMA) ligands have also been conjugated with one or two bioreductive moieties in order to improve the physicochemical properties of hypoxia markers [45]. The key reagent, MAMA-amino acid (MAMA-AA) was prepared starting with the reaction of MAMA with ethylbromoacetate to afford the ethyl ester, which was saponified and acidified to obtain MAMA-AA. The corresponding mono-4-nitroimidazole and 2-nitroimidazole (MAMA-AA-4NI and MAMA-AA-2NI) compounds (ligands for complexes **55**, **56**; Figure 19) were synthesized by coupling MAMA-AA with the corresponding amino derivative of 4- or 2-nitroimidazole in the presence of BOP as a condensation agent. For the MAMA-bis-4-nitroimidazole and 2-nitronimidazole (ligands for complexes

ISSN: 2057-3782 (Online)
http://dx.doi.org/10.17229/jdit.2015-0415-015

53, **54**; Figure 19) compounds, it was necessary to form the aminofunctional bis(nitroimidazole) intermediates for direct coupling in the presence of BOP, followed by thiol group deprotection with ethanolic HCl at 100 °C.

Radiolabelling was performed *via* tin(II)-mediated reduction of ^{99m}Tc-glucoheptanoate. The ^{99m}Tc-labelled MAMA nitroimidazole derivatives (**53-56**), prepared with over 95% radiochemical purity, were stable *in vitro* in rat serum for 4 h at 37 ˚C. With log*P* values of 0.12, 0.28, 0.61 and 0.69 (**53-56**, respectively), they are less lipophilic than BMS181321 (**19;** log*P* 1.59). Biodistribution studies in Kunming mice bearing murine sarcoma tumours (S180) revealed lower radioactivity in liver and more rapid clearance from blood for the MAMA-bisnitroimidazoles compared to the corresponding mononitroimidazole derivatives. T/B and T/M ratios at 4 h for the ^{99m}Tc-bis(nitroimidazole) complexes **53** (0.73 and 3.23, respectively) and **54** (0.70 and 2.68, respectively) were higher than those of mononitroimidazole counterparts **55** (T/B 0.77, T/M 2.17) and **56** (T/B 0.81, T/M 2.83). Additionally, the complexes with single 2-nitroimidazole or 4-nitroimidazole groups showed higher T/B than ^{99m}Tc-BMS181321 (**19**) [45].

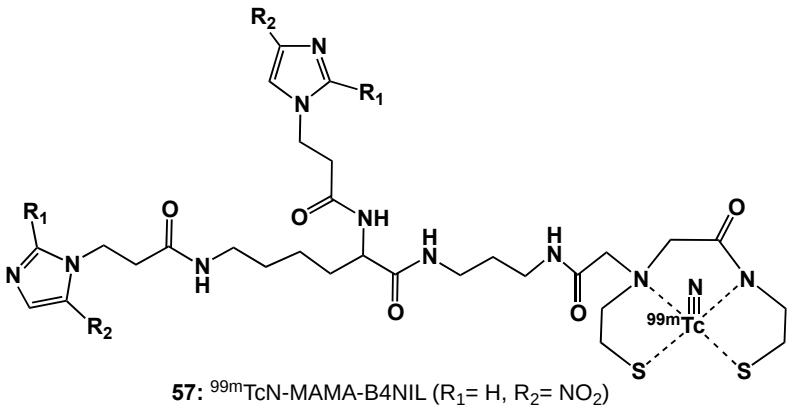

Figure 20. Monoamine-monoamide dithiol ligands complexed with ^{99m}Tc-nitrido core.

Additional studies using MAMA-bisnitroimidazole derivatives as chelating ligands were based on the isoelectronic $[^{99m}TcN]^{2+}$ (**57**, **58**; Figure 20) instead of the $[^{99m}TcO]^{3+}$ metal core [71]. This Tc-nitrido core has demonstrated high affinity with chelating ligands having S donor atoms, and it is a good π-electron donor that provides stability to Tc^{5+} oxidation state. The $[^{99m}TcN]^{2+}$ core was prepared from $[^{99m}TcO_4]^-$ using succinic dihydrazide (SDH) as the nitride precursor in the presence of $SnCl_2$. Both complexes retained radiochemical purity of 98% for up to 4 h *in vitro.* They exhibited low protein binding and were more hydrophilic than their corresponding Tc-O counterparts (**57**: log*P* -2.56; **58**: log*P* -2.49). Biodistribution studies in S180 sarcomas-bearing male Kunming mice showed rapid radioactivity clearance from blood and soft tissues, and hepatobiliary excretion. Compared with the ^{99m}Tc-oxo-bisnitroimidazoles in the same tumour model, ^{99m}Tc-nitrido-bisnitroimidazole complexes exhibited greater potential for tumour hypoxia targeting with their better T/B and T/M ratios. Compound

ISSN: 2057-3782 (Online)
http://dx.doi.org/10.17229/jdit.2015-0415-015

57, at 2 h post-injection, attained T/B and T/M values of 3.05 and 5.27, respectively, compared to **58**, with respective ratios of 1.16 and 4.24, respectively.

3.3.10. Technetium 2,2',2"-nitrilotris(ethanethiol) and isocyanide (4+1) nitroimidazoles

The ^{99m}Tc-based mixed ligand radiopharmaceuticals (**59, 60**; Figure 21) have a coordination sphere that consists of the metal centre, a tetradentate 2',2"-nitrilotris(ethanethiol) and a monodentate isocyanide-metronidazole derivative, forming a trigonal bipyramidal geometry [46]. The isocyanide-metronidazole derivatives such as 4-isocyano-*N*-[2-(2-methyl-5-nitro-1*H*-imidazol-1-yl)ethyl]butanamide (M1) and 1-(4-isocyanobutanoyl)-4-[2-(2-methyl-5-nitro-1*H*-imidazol-1-yl)ethyl]piperazine (M2) (Figure 21) were obtained by the reaction between the corresponding amino-functionalized metronidazole and the succinamide derivative of 4-isocyanobutanoic acid. In a separate synthesis, the tripodal ligand was prepared starting with tris(2-chloroethyl)amine hydrochloride and potassium thioacetate in ethanol. Labelling through the formation of the mixed tetradentate-monodentate (4+1) complex was performed by substitution using the ^{99m}Tc-EDTA/mannitol precursor (EDTA= ethyldiaminetetraacetic acid), which was obtained by means of the standard reduction of $^{99m}TcO_4^-$ using stannous chloride.

Complexes **59** and **60** were obtained in quantitative yields with > 90% radiochemical purity and were stable for 6 h in the labelling milieu and for 4 h in human plasma. Complex **59** was less lipophilic (log*P* 0.77) and displayed low protein-binding, compared to **60** (log*P* 1.2) which was more highly protein bound. Using human adenocarcinoma HCT-15 cells, HSF values for **59** and **60** were 1.5 and 1.4, respectively. Biodistribution in C57BL/6 mice inoculated with 3LL murine Lewis lung carcinoma cells revealed high initial tumour uptake and significant retention of **59** at 4 h post-injection. Clearance from background tissue was fast, with moderate T/M and T/B ratios (2.0 and 1.0, respectively) at 4 h post-injection [46].

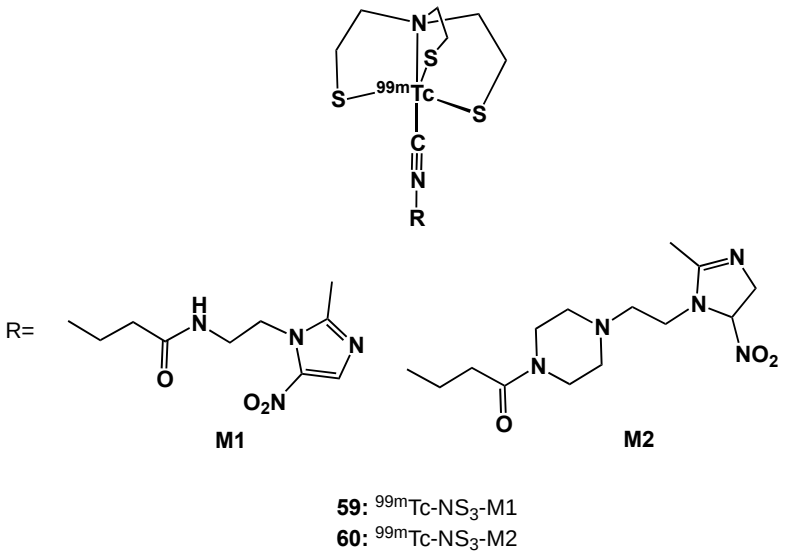

Figure 21. ^{99m}Tc complexes with mixed 4+1 ligands.

ISSN: 2057-3782 (Online)
http://dx.doi.org/10.17229/jdit.2015-0415-015

3.3.11. Technetium ligands containing PEG linked nitroimidazoles

In complexes **61**-**63** (Figure 22), the 2-nitroimidazole moiety has been modified through the incorporation of a polyethylene glycol (PEG) linker, a process known as "pegylation". This approach has been found to be very useful in the preparation of radiopharmaceuticals in order to improve their *in vivo* stability and pharmacokinetics, thereby enhancing their therapeutic potential. Pegylated-nitroimidazole was conjugated to tridentate bifunctional chelators such as bis-2-pyridinylmethanamine (BPA), 2-picolylamine-N-acetic acid (AOPA) and iminodiacetic acid (IDA) [72]. The amino-functional-pegylated nitroimidazole, 2-(2-(2-(2-(2-nitro-1*H*-imidazol-1-yl)ethoxy)ethoxy)ethoxy)-ethanamine was reacted with 2-chloromethyl pyridine hydrochloride to form BPA-PEG_3-NIM. The same starting material was treated with *tert*-butyl bromoacetate and Na_2CO_3 to convert the amine to ester groups, which were hydrolysed with HCl to give the IDA-PEG_3-NIM ligand. The synthesis of PAA-PEG_3-NIM involved 3 steps starting with the 2-(2-(2-(2-(2-nitro-1*H*-imidazol-1-yl)ethoxy)ethoxy)ethoxy)ethyl-4-methylbenzensulfonate as a precursor. Radiolabelling of these ligands with $[^{99m}Tc(CO)_3]^+$ afforded the complexes in 95% yield. The log*P* values of **61**, **62** and **63** were -1.11, -0.44 and -1.64, respectively.

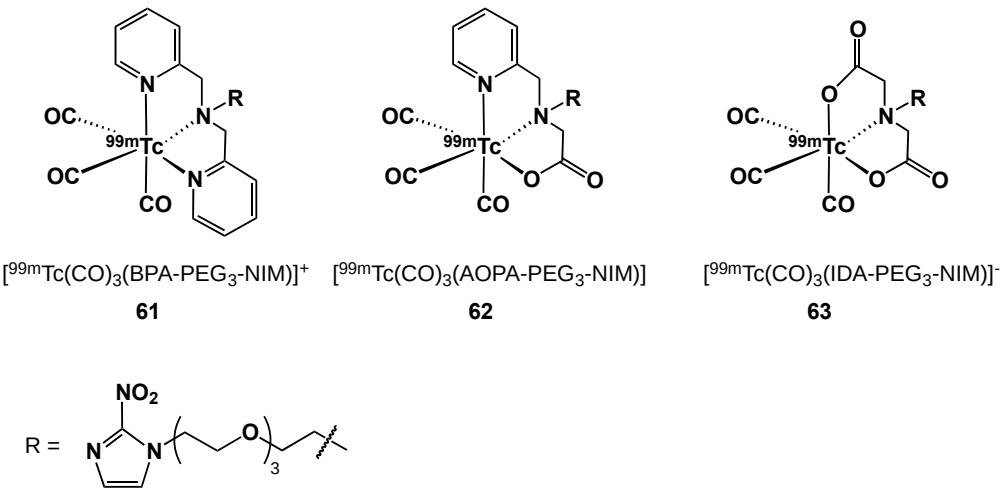

Figure 22. ^{99m}Tc complexes with the incorporation of PEG as a linker.

Biodistribution studies in Kunming mice bearing S180 cancer xenografts showed that all the three complexes were excreted *via* both renal and hepatobiliary routes; their clearance from normal organs was not fast, thus leading to high backgrounds 2 h p.i. Complexes **61** and **62** had comparable tumour targeting affinity, which was better than **63**. On the other hand, the T/M ratios of **62** and **63** (0.14 and 0.26, respectively) at 2 h p.i. were lower than that of **61** (0.61) [72].

ISSN: 2057-3782 (Online)
http://dx.doi.org/10.17229/jdit.2015-0415-015

3.3.12. Technetium xanthate nitroimidazoles

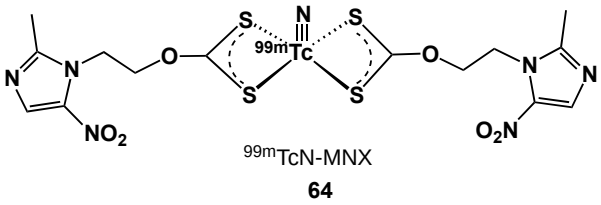

Figure 23. Bismetronidazole ^{99m}Tc-xanthate complexes.

Metronidazole xanthate was utilized in the design of the first xanthate-based ^{99m}Tc complex (**64**, Figure 23) as a target agents for hypoxia [73]. It was synthesized by adding carbon disulfide to a solution of metronidazole and sodium hydroxide to give the sodium salt metronidazole xanthate. The technetium-nitrido core $[^{99m}TcN]^{2+}$ was prepared from $^{99m}TcO_4^-$. Maximum complexation of **64** (95%) was achieved at room temperature with low ligand concentration. Complex **64** was stable for over 20 h, with 85% radiochemical purity, and it retained 90% radiochemical purity in serum after 3 h. The complex was found to be neutral upon analysis by paper electrophoresis.

Biodistribution studies in Swiss mice bearing transplanted fibrosarcoma tumours showed steady retention of radioactivity in tumours throughout the 3 h period. T/B and T/M improved steadily with time and were 0.62 and 3.3; respectively at 3 h post-injection. Time-dependent clearance from other vital organs coincided with hepatobiliary excretion [73].

3.3.13. Peptide-based technetium nitroimidazoles

Peptidic N_3S chelator backbones prepared by automated solid phase synthesis were coupled to 2-nitroimidazole to afford *L*-seryl-*L*-cysteinyl-lysyl[N_ε[1-(2-nitro-1*H*-imidazolyl)acetamido]]glycine (RP435) and dimethylglycyl-*tert*-buylglycyl-*L*-cysteinyl-glycine-[2-(2-nitro-1*H*-imidazolyl)ethyl]-amide (RP535; Figure 24) [74]. Radiolabelling of RP435 was carried out at room temperature *via* transchelation from ^{99m}Tc-gluconate under reducing conditions to form complex **65**. HPLC analysis showed two peaks, indicating the existence of both *syn*- and *anti*- conformations with respect to the ^{99m}Tc-oxo bond and serine hydroxymethyl side chain.

The presence of the bulky *tert*-butyl group in RP535 required chelation to be performed at higher temperature (60-100 ^{0}C), which provided exclusive formation of a single conformation of the complex and increased its lipohilicity (log*P* 0.45), when compared to the two isomers of **65**, which had log*P* values of -3.05 and -2.96. The radiochemical yield of **66** was 78%, compared to that of **65** (68%). Furthermore, **66** was more stable than **65** at room temperature in aqueous solution containing 0.1% TFA,

ISSN: 2057-3782 (Online)
http://dx.doi.org/10.17229/jdit.2015-0415-015

with no decomplexation or change in radioactivity for 26 h. The HSF of **66** in CHO cells was greater than that for **65** [74].

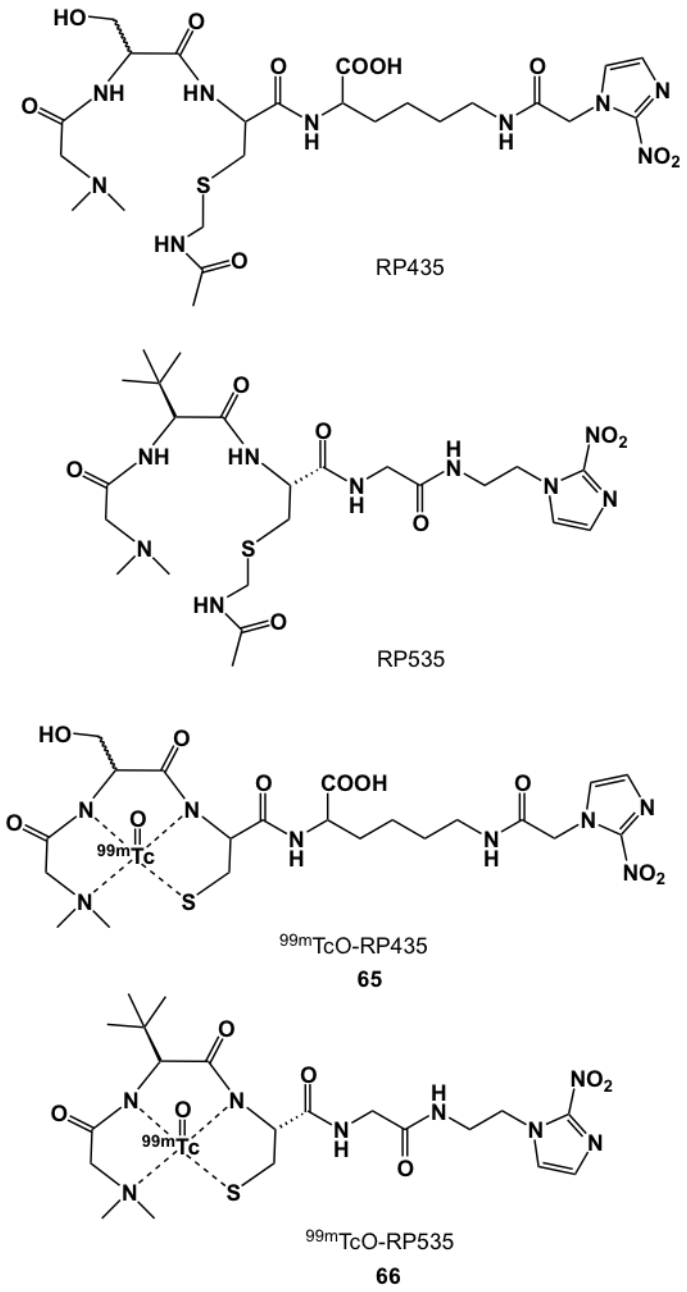

Figure 24. ^{99m}Tc-labelled peptidic 2-nitroimidazoles.

ISSN: 2057-3782 (Online)
http://dx.doi.org/10.17229/jdit.2015-0415-015

Other peptides linked to 2-nitroimidazole include 1-[(diphenylphosphino)acetylglycylglycyl-2-aminoethyl]-2-nitroimidazole (HL-501) and 1[*N*-benzoyl-thioglycolyl)glycylglycyl-2-aminoethyl]-2-nitroimidazole (HL-601) (Figure 25) [75]. These ligands were synthesized *via* condensation between 1(*N*-glycylglycyl-2-aminoethyl)-2-nitroimidazole hydrochloride and the corresponding carboxylic acid. In the presence of a reducing agent and [Na][$^{99m}TcO_4$], the peptidic chelators formed **67** and **68**, respectively as neutral complexes in high radiochemical yields. Biological assessment and imaging studies performed on Balb/c mice bearing EMT-6 tumours showed negligible tumour uptake.

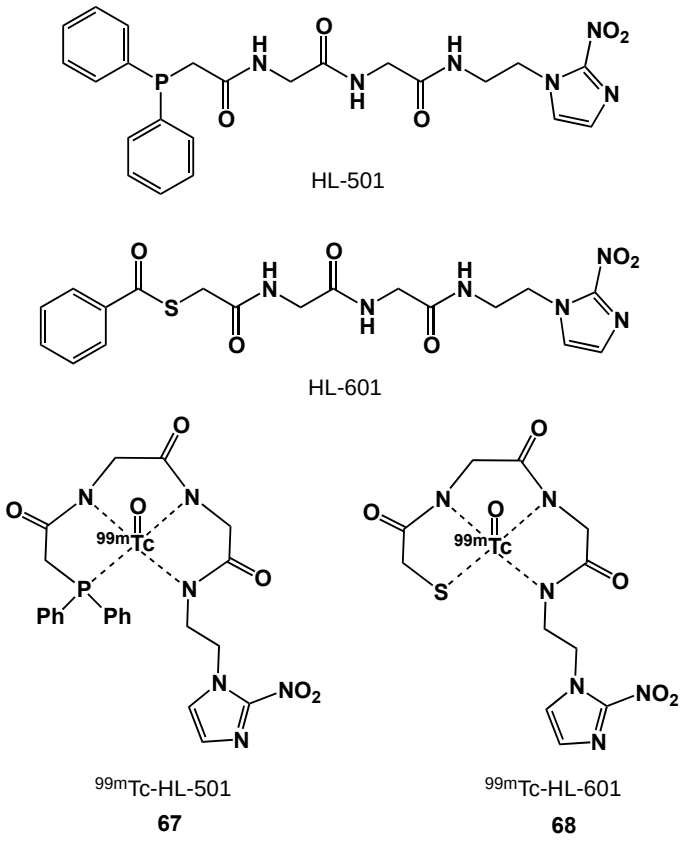

Figure 25. ^{99m}Tc-labelled diphenylphoshino/mercapto peptide-2-nitroimidazole conjugates.

4. Lanthanide metal - nitroimidazole complexes

4.1. Gadolinium nitroimidazole complexes

Gadolinium is a lanthanide with 6 stable isotopes, $^{154\text{-}158}$Gd, and ^{160}Gd. None of the radioisotopes are suitable for diagnostic nuclear medicine, but ^{155}Gd and ^{157}Gd (both have a natural abundance of ~15%) have nuclear spins of 3/2, making them useful in NMR/magnetic resonance imaging (MRI), and their high neutron capture cross sections make them attractive targets for neutron capture therapy [76].

ISSN: 2057-3782 (Online)
http://dx.doi.org/10.17229/jdit.2015-0415-015

Gadolinium-153 decays by electron capture ($t_{1/2}$ 240 d) [77], and with relatively soft gamma emissions of 69.67 (2.44%), 97.43 (21.6%) and 103.18 (29.5%) keV [78], has been used as an agent for bone density measurements. The most common oxidation state is +3, which has an ionic radius of 0.99Å, similar to Ca^{2+}. Typical ligands have eight donor atoms, leaving a single water atom in its inner coordination sphere [79].

A gadolinium-based 2-nitroimidazole derivative was developed and evaluated for its potential to detect hypoxic cells by MRI [80]. The target chelator was synthesized *via* acid-amine coupling between DO3A-monobutylamide (DO3A= 1,4,7,10-tetraazacylododecane-1,4,7-tri(acetic acid *tert*-butyl ester)) and nitroimidazolyl hexanoic acid. The protected DO3A-monoamide derivative was prepared by alkylating the DO3A-tris(*tert*-butyl ester) precursor with methylchloroacetate, and the resulting intermediate was treated with diaminobutane.

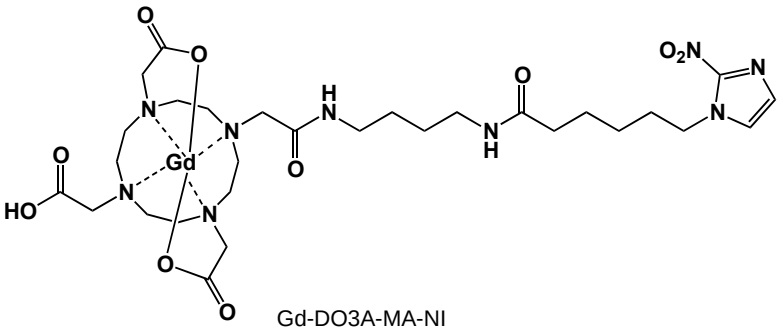

Figure 26. The gadolinium-nitroimidazole complex, Gd-DO3A-MA-NI (69), for targeted hypoxia studies by MRI.

The 2-nitroimidazole vector was synthesized by the reaction between 2-nitroimidazole and ethylbromohexanoate. The ligand design included an extended linker in order to ensure favourable lipophilicity and prevent interference with the coordination environment by the nitroimidazole moiety. The Gd(III) centre is chelated by the 4 *N* macrocyclic donor atoms and 3 *O* atoms from the carboxylate and the amide pendant groups of 1,4,7,10-tetraazacyclododecane-1,4,7-tri(acetic acid)-10-acetic acid *N*-(4-aminobutyl-6-(2-nitro-1*H*-imidazol-1-yl)hexanamide amide (**69**; Figure 26). This complex was thermodynamically stable, although less so than the corresponding anionic Gd-DOTA, in which all carboxylic groups were fully deprotonated. Its feasibility as a hypoxia MRI probe was assessed in rat 9L glioma cells, where it was found to be selectively trapped in hypoxic tissues.

ISSN: 2057-3782 (Online)
http://dx.doi.org/10.17229/jdit.2015-0415-015

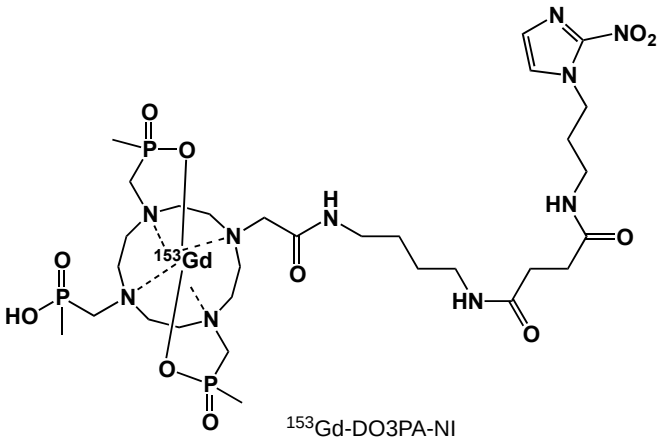

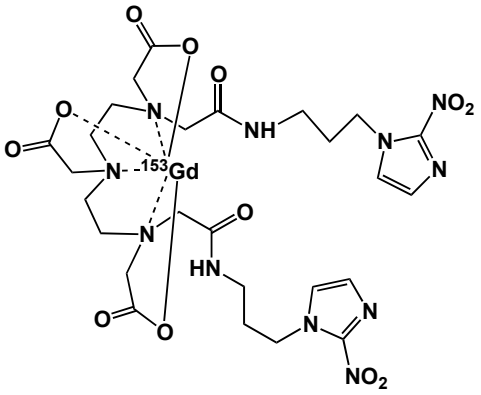

Figure 27. ^{153}Gd complexes of DO3PA-nitroimidazole (70) and DTPA-nitroimidazole (71).

The bifunctional hexadentate ligand, 1,4,7,10-tetraazacyclododecane-1,4,7-tri-[(methylene)-methylphosphonic acid] (DO3PA) was prepared and conjugated to a nitroimidazole derivative [81]. The effective route for the synthesis of the trismethylenephosphonate chelator involved the reaction of molybdenum hexacarbonyl to cyclen in dibutyl ether, resulting in the formation of a molybdenum-cyclen-tricarbonyl complex [82].

Selective mono-*N*-alkylation preceded by the addition of α-bromoamide, and after decomplexation of the complex in aqueous acid, the methyl phosphinate groups were introduced and subsequently hydrolysed to give the trisphosphinic acid. The pendant amino functionality was converted to an active ester, which allowed the facile conjugation of 1-aminopropyl-2-nitroimidazole to form DO3PA-NI. Radiolabelling with ^{153}Gd provided a neutral complex that was stable *in vivo*. The biodistribution of **70** (Figure 27) was examined in normal mice. There was no selective build-up in hypoxic tissues, and the complex rapidly cleared renally, so that after 24 h less than 1% of radioactivity was retained [82].

ISSN: 2057-3782 (Online)
http://dx.doi.org/10.17229/jdit.2015-0415-015

An acyclic diethylenetriaminepentaacetic acid-nitroimidazole conjugate (DTPA-NI) was also labelled with ^{153}Gd (**71**) [81]. Its biodistribution in immunocompromised mice bearing a xenograft of KHT sarcoma tumour showed T/B ratios of 0.27 and 0.076 at 4 h and 24 h post-injection, respectively, with slow blood clearance. No significant tumour localization was observed, and radioactivity was high in bone. These results were attributable to the dianionic charge of the complex, resulting in poor *in vivo* stability [81].

4.2. Lutetium nitroimidazole complexes

Lutetium-177 has proven potential for the detection and measurement of hypoxia owing to its ideal nuclear characteristics [83]. This isotope decays with a half-life of 6.71 days by beta particle emission ($E_{\beta max}$ 497 keV; 78.6%) and several gamma rays ($E_{\gamma max}$ 113 keV, 6.4.6%; 208 keV 11%). It can also be produced in high radiochemical and radionuclidic purity after thermal neutron bombardment of the unlabelled precursor. Reported nitroimidazole-based hypoxia markers incorporating ^{177}Lu are based on 1,4,7,10-tetraazacyclododecane-1,4,7,10-tetraacetic acid (DOTA), a twelve-membered tetraazamacrocycle containing four pendant carboxylic acids tethered to a cyclen amine that can be derivatized and coupled to nitroimidazole-containing moieties while the nitrogen atoms and the remaining carboxylate groups coordinate with a metal centre.

Three ^{177}Lu-DOTA nitroimidazoles have been reported (Figure 28). The (*N*-(2-methoxyethyl)-3-nitro-1*H*-1,2,4-triazole-1-acetamide) conjugate (**72**) was synthesized after a one-step coupling between the sanazole derivative and *p*-amino-DOTA-anilide [84]. Radiolabelling proceeded by adding $^{177}LuCl_3$ in ammonium acetate buffer at pH 5. The extent of complexation as determined by paper chromatography was >99%, and the radiochemical yield could be optimized to 97.8%. Complex **72** was relatively stable at room temperature up to 7 days after radiolabelling. Its biodistribution in Swiss mice bearing fibrosarcoma tumours was characterized by high renal clearance and T/B ratios of 4.0, 4.3 and 18.0 at 1 h, 3 h and 24 h post-injection, respectively. The respective T/M ratios were 4.6, 10.7 and 18.0 at the corresponding times.

The *p*-aminobenzyl-DOTA-metronidazole conjugate was synthesized starting with the oxidation of MN to 2-[*N*-(2'-methyl-5'-nitro)imidazolyl]ethanoic acid [85]. The addition of $^{177}LuCl_3$ to the solution containing MN-*p*-aminobenzyl-DOTA afforded **73** in 97% radionuclidic purity and yield. The complex exhibited excellent stability for up to 10 d at room temperature. Biodistribution studies in Swiss mice bearing fibrosarcoma tumours revealed good tumour uptake with favourable T/B (5.2 at 1 h and 28.0 at 24 h p.i.) and T/M ratios (12.2 at 1 h and 14.0 at 24 h post-injection) [85].

A solid-phase strategy for the synthesis of ^{177}Lu-DOTA-NI (**74**) involved introducing the chelating agent to amino acid-Wang resin after selective deprotection of the lysine side-chain by trifluoroacetic acid [86]. Fmoc cleavage with 20% piperidine enabled the coupling of 2-NI with the DOTA-Lys-Wang resin and under TFA:TIS:EDT:thioanixole:water released the DOTA-Lys-nitroimidazole conjugate.

ISSN: 2057-3782 (Online)
http://dx.doi.org/10.17229/jdit.2015-0415-015

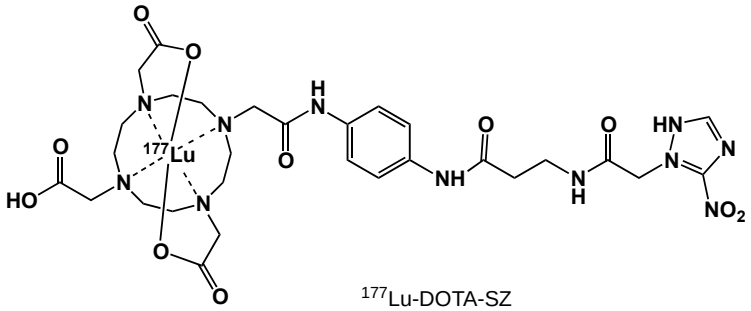

^{177}Lu-DOTA-SZ
72

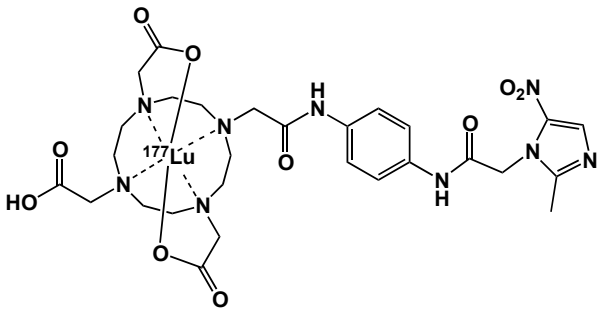

^{177}Lu-DOTA-MN
73

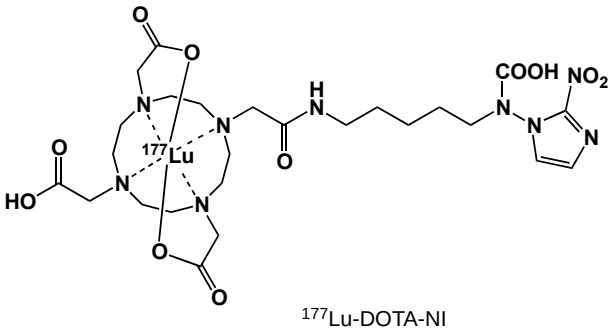

^{177}Lu-DOTA-NI
74

Figure 28. ^{177}Lu-labelled DOTA nitroimidazole derivatives (**72-74**).

For the radiolabelling, a solution containing the conjugate, ascorbic acid and dihydrobenzoic acid in sodium acetate buffer (pH 5.5) was mixed with ^{177}Lu and heated. In female mice bearing subcutaneously implanted human lung cells, **74** was rapidly taken up by the kidneys and excreted *via* the urine; no additional animal data are provided [86].

5. Main group metal - nitroimidazole complexes

5.1. Aluminium nitroimidazole complexes

The reported aluminium coordination compounds are unique because the metal centre is not the radioactive element but is used to bind the ^{18}F radionuclide [87]. These compounds have no

ISSN: 2057-3782 (Online)
http://dx.doi.org/10.17229/jdit.2015-0415-015

radiotherapeutic potential but offer an interesting approach to the synthesis of unique radiofluorinated organometallic complexes. The labelling approach is straightforward and eliminates multiple steps in purification and evaporation, which improves overall recovered radiochemical yield. The reported Al-^{18}F complexes exploit 2-NI derivatives of 1,4,7-triazacyclononane-*N,N'*-diacetic acid (NODA) as the chelating core (**75**, **76**; Figure 29). The NODA-NI conjugates were prepared by reaction of 2-NI with a 2-carbon or 3-carbon linker (1,2-dibromoethane or 1,3-dibromopropane) in the presence of K_2CO_3 base, followed by coupling the resulting derivatives with NODA^{t}Bu and deprotecting with base to afford the NODA-NI1 and NODA-NI2 ligands. Al[^{18}F]fluoride complexes (**75, 76**) were prepared by mixing [^{18}F]fluoride and $AlCl_3$ in a buffer solution at pH 4 at room temperature, followed by reaction with the NODA-nitroimidazole ligands to obtain either complex in >80 % radiochemical yield and 99% radiochemical purity. The non-radioactive products were stable in serum and exhibited low (<1 %) protein binding *in vitro*.

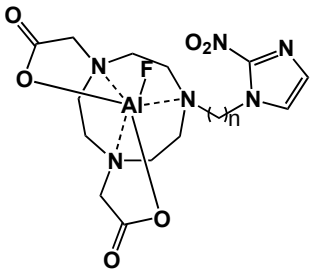

75: Al^{18}F-NODA-NI1, n= 2
76: Al^{18}F-NODA-NI2, n= 3

Figure 29. Aluminium-^{18}F NODA-NI complexes.

The HSF for **75** and **76** in HeLa, CHO and CT-26 cells ranged from 3.9 to 10 after a 1 h incubation [88]. Biodistribution studies in a mouse colon cancer CT-26 xenograft balb/c mice model showed early uptake by liver, kidney and hypoxic cancer cells (~0.23 % injected dose at 100 min), and rapid clearance from blood. The highest T/M and T/B ratios were obtained at 1 h post-injection, with T/M values of 14.5 (1 h) and 0.5 (2 h) for **75**, and 37.4 (1 h) and 0.5 (2 h) for **76**. The rapid rise and fall in tumour to non-tumour concentration ratios were indicative of rapid perfusion-equilibration with limited selective bioreductive binding, but tumours were delineated in small animal PET images.

5.2. Gallium nitroimidazole complexes

The most commonly used PET tracers for imaging tumour hypoxia are labelled with radionuclides of fluorine (^{18}F), copper (^{64}Cu) and iodine (^{124}I), while SPECT agents are predominantly radioiodines $^{123/131}$I and ^{99m}Tc [89-90]. Gallium, traditionally among the less frequently used tracers, has experienced a general renaissance following the advent of functional, commercially available ^{68}Ga generators. Gallium has two stable ($^{69/71}$Ga) and numerous radioactive isotopes, of which ^{67}Ga and ^{68}Ga are of interest in nuclear medicine. Gallium-67 decays *via* electron capture with gamma rays at 73 – 393 keV

ISSN: 2057-3782 (Online)
http://dx.doi.org/10.17229/jdit.2015-0415-015

and $t_{1/2}$ of 78 h, whereas ^{68}Ga decays by positron emission (89%; E_{max} 1899 keV) and electron capture (11%) with $t_{1/2}$ 67.7 min.

In aqueous solution, gallium complexes predominantly exist in the third oxidation state (Ga^{3+}) [91]. Oxidation and reduction of Ga^{3+} do not occur under physiological conditions, but in the 3-7 pH range; hydrolysis can lead to precipitation of $Ga(OH)_3$, which dissolves at pH>7 as $[Ga(OH)_4]^-$. During the radiolabelling process, the formation of these species is problematic since the kinetics for substitution of the hydroxide ligands is rather slow, rendering coordination of multidentate ligands difficult. To circumvent this problem, ligand-exchange reaction is performed in the presence of weakly coordinating ligands such as citrate, acetate or oxalate. According to the hard and soft acids and bases (HSAB) principle, Ga^{3+} is classified as a hard Lewis acid due to its high charge density and small ionic radius (0.62 Å). As a consequence, chelation is characterized by the preference to highly ionic, non-polarizable hard Lewis bases such as nitrogen and oxygen donor atoms. These include ligands with carboxylate, phosphonate, hydroxamate and amine functionalities form thermodynamically stable complexes. Due to its small cationic radius, the coordination sphere of Ga^{3+} often assumes a six-coordinate distorted octahedral geometry; however, four- and five-coordinate complexes also form.

Gallium(III) chelates have high thermodynamic stability and kinetic inertness to avoid premature ligand-exchange reactions or hydrolysis *in vivo*. Complete saturation of the coordination sphere of Ga(III) is desirable because coordinatively unsaturated complexes are generally more prone to ligand exchange or hydrolysis. Consequently, polydentate ligands with hard donor groups remain first choice for gallium labelled biomolecules. Among these are the nitroimidazole derivatives of bifunctional chelators such as 1,4,7-triazacyclononane-1,4,7-triacetic acid (NOTA) and 1,4,7,10-tetraazacyclododecane-1,4,7,10-tetraacetic acid (DOTA) (Figure 30).

The ligand of choice for ^{67}Ga-NOTA-1 (**77**), was synthesized starting with the active ester and the aminolalkyl nitroimidazole [81, 92]. Radiolabelling was performed *via* complexation of the ligand with the ^{67}Ga salt. In Chinese hamster fibroblasts under hypoxic conditions, the ratio of radioactivity in the cells to that in the medium was 0.8:1, close to that of the analogous non-nitroimidazole containing ^{67}Ga-NOTA complex (0.99:1). Two other NOTA derivatives, **78** and **79** were prepared, all with radiolabelling efficiencies of 96% [93]. Complex **78** (log*P* -2.71) was more hydrophilic than **79** (log*P* -2.27), attributed to the absence of the aromatic ring in the former compound.

Both agents showed low protein binding and were stable up to 4 h at room temperature. Crystallographic studies showed that the coordination sphere consisted of the Ga^{3+} centre, three *N* atoms (from the macrocycle) and three O atoms (two from the pendant COOH groups and one from the amide group), forming a distorted octahedral geometry. HSF values after 1 h incubation with CHO and CT-26 cell lines were 1.8 and 1.5, respectively for **78**, and 5.6 and 2.6, respectively, for **79**, comparable to those of ^{18}F-FAZA (1.4 at 20 min and 2.7 at 100 min) and ^{18}F-FMISO (1.5 at 20 min and 3.0 at 100 min).

ISSN: 2057-3782 (Online)
http://dx.doi.org/10.17229/jdit.2015-0415-015

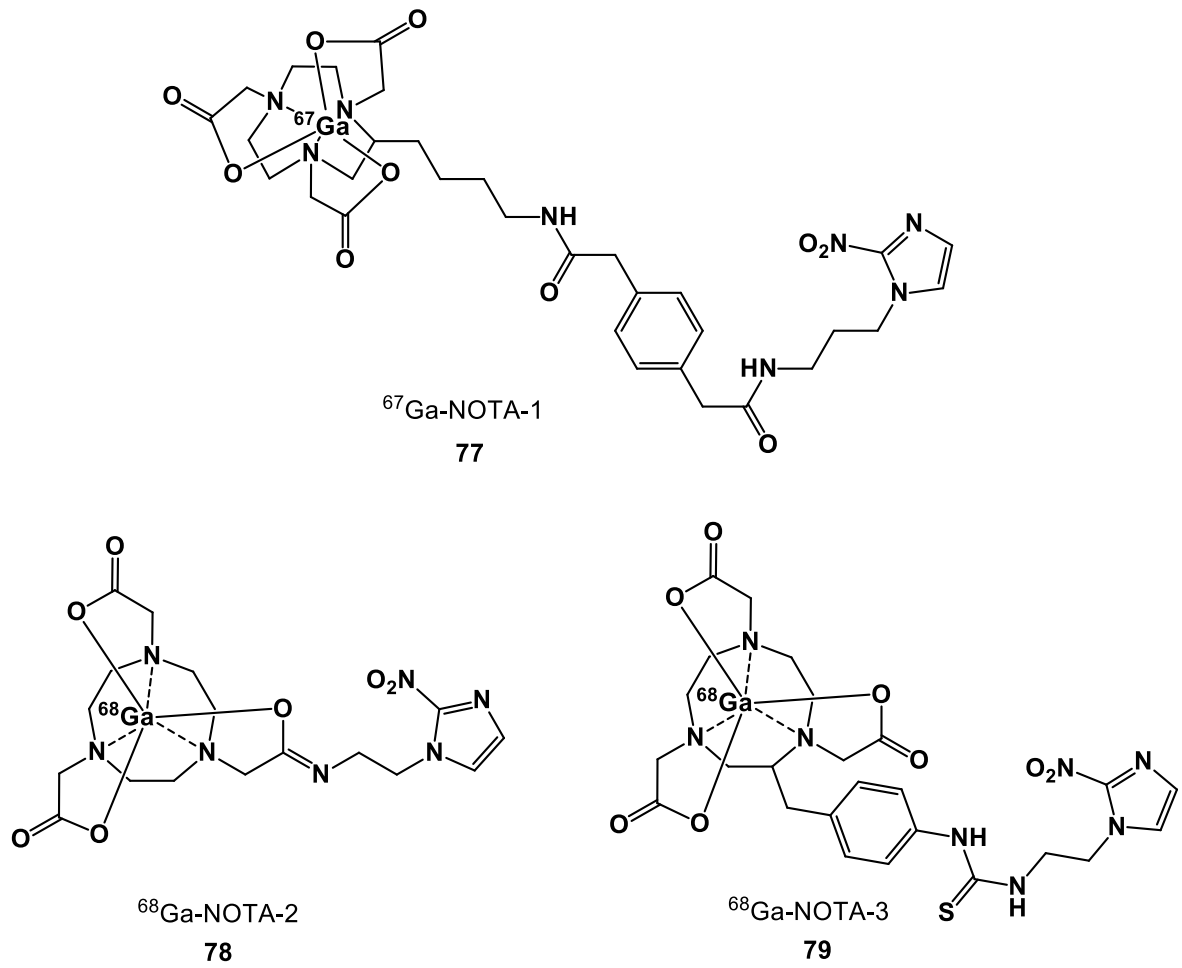

Figure 30. NOTA-based $^{67/68}$Ga nitroimidazole complexes (**77-79**).

After intravenous injection in CT-26 xenografts-bearing mice, the labelled compounds displayed prominent kidney, liver and intestinal uptakes with higher values for **79** than **78**; T/B ratios for **78** and **79** at 1 h post-injection were 0.6 and 0.7, respectively. At the same time point, the T/M ratios were 2.1 and 1.6. PET images confirmed the biodistribution study data [93].

To increase the hydrophilicity of ^{68}Ga-labelled hypoxia imaging agents, 2-(2-nitroimidazolyl)ethyl amine HCl salt was alternatively conjugated to DOTA and DOTA-SCN (**80**, **81**; Figure 31) [94]. Labelling efficiencies for the complexes were up to 98%, both products were stable in human serum and more hydrophilic than their NOTA counterparts (**80** log*P* -4.60; **81** log*P* -4.5). The HSF ratios for **80** in HeLa, CHO and CT-26 after 1 h were 2.4, 1.8 and 6.8; respectively, while values obtained for **81** were 2.1, 2.3 and 3.4. Biodistribution studies in CT-26 xenografts-bearing mice showed T/M ratios at 2 h post-injection of 3.96 for **80** and 12.5 for **81**. At the same time points, the corresponding T/B values for **80** and **81** were ~0.9 and ~1.5, respectively. The more lipophilic **81** complex showed higher liver uptake,

ISSN: 2057-3782 (Online)
http://dx.doi.org/10.17229/jdit.2015-0415-015

but higher standard uptake values in tumours were recorded for **80**. Complex **80** demonstrated more distinct PET images than **81**.

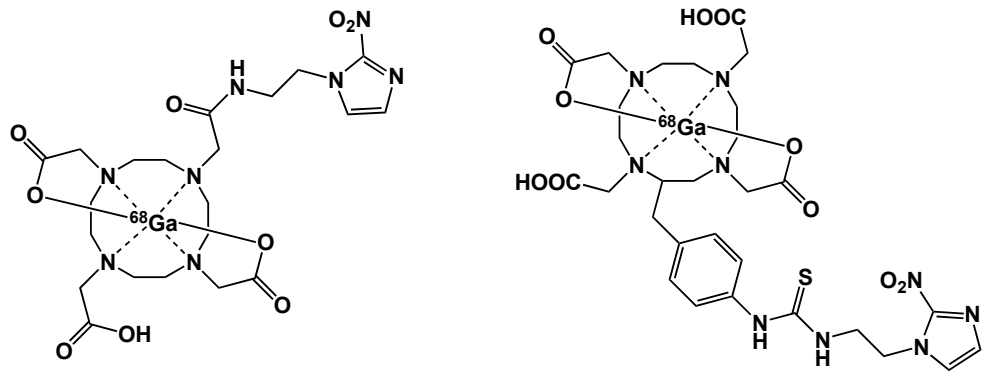

^{68}Ga-DOTA-1 **80** ^{68}Ga-DOTA-2 **81**

Figure 31. DOTA-2-nitroimidazole-based $^{67/68}$Ga complexes.

On the basis that Ga^{3+}-DOTA complexes form hexacoordinated structures, two metronidazole moieties were conjugated to the DOTA bifunctional chelator (Figure 32) [95]. ^{68}Ga-DOTA-MN2 (**82**) was prepared by heating a solution of the ligand with a non-radioactive gallium precursor, $Ga(NO)_3.xH_2O$ in ammonium acetate buffer (pH=4.6). In order to validate the synthetic utility of the design, the DOTA-MN was radiolabelled with ^{67}Ga-citrate in an ammonium acetate buffer (pH 5.8) at 95 ^{0}C. Complex **83** was obtained in 35-59% radiochemical yields with over 96% radiochemical purity. The complex was stable *in vitro* during a 24 h incubation in phosphate-buffer and mouse plasma solutions. In NFSa tumour-bearing C3H/He mice, **83** displayed significant tumour uptake, fast blood clearance and high target to non-target ratios; its T/B and T/M ratios peaked at 6 h post-injection with values of 4.5 and 4.4, respectively. Overall, the results suggested that two metronidazole moieties conjugated with the radiogallium-DOTA centre did not reduce *in vitro* and *in vivo* stabilities and offered significant improvements in recognition of hypoxic sites by the biomarker [95].

Based on promising preliminary animal studies with **83** [95], improved radiochemical yield (85%) and radiochemical purity (99%) were achieved using microwave-assisted reaction [96]. The effectiveness of the two metronidazole moieties in **83** was compared to the complex bearing only one metronidazole (**84**). Complex **83** showed significant accumulation in hypoxic regions in FM3A carcinomas. Heterogeneous distributions of **84** within both NFSa and FM3A tumours were confirmed using *ex vivo* autoradiography.

ISSN: 2057-3782 (Online)
http://dx.doi.org/10.17229/jdit.2015-0415-015

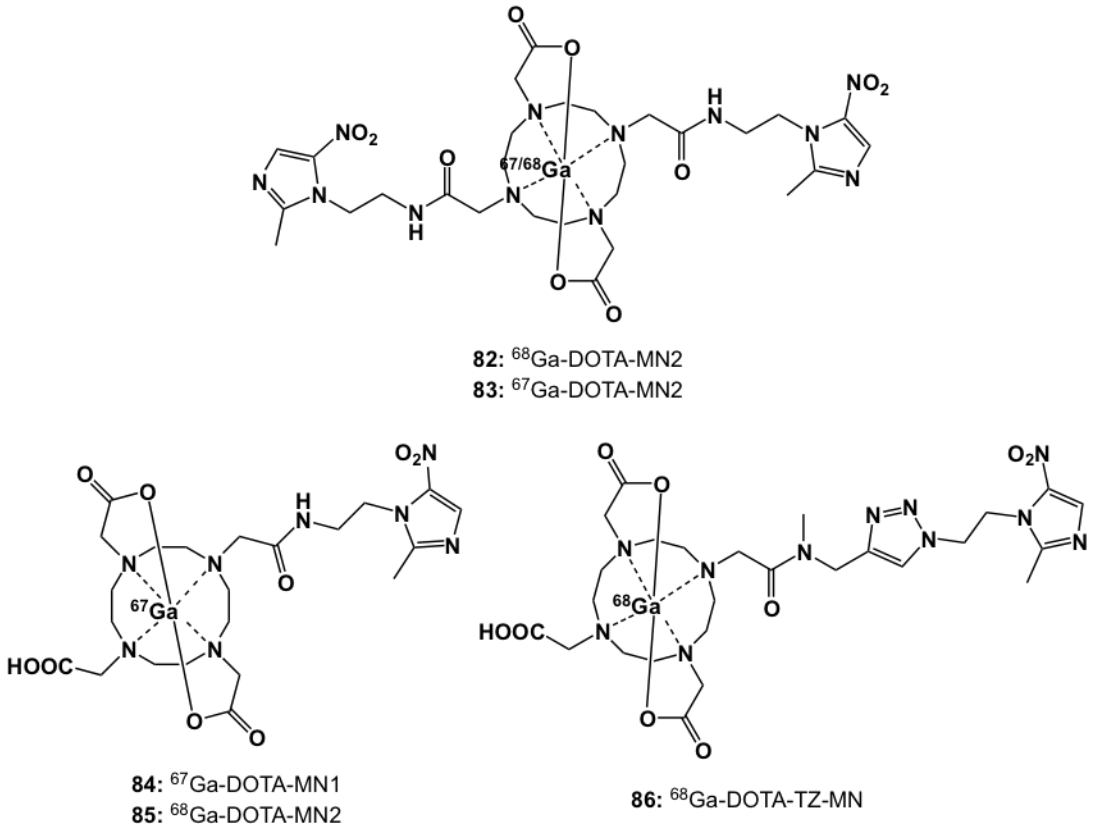

Figure 32. $^{67/68}$Ga chelated with bismetronidazole-DOTA (**82**, **83**) monometronidazole-DOTA (**84, 85**) and DOTA-triazole-metronidazole (**86**) derivatives.

Biodistribution of radioactivity in mice implanted with FM3A breast tumours showed that **83** provided higher T/B ratios (7.2 at 3 h and 6.2 at 6 h post-injection) than **84** (3.3 at 3 h and 2.9 at 6 h post-injection). A similar trend was observed for the T/M ratios of **83** (18 at 3 h and 8.3 at 6 h post-injection) and **84** (9 at 3 h and 4.6 at 6 h post-injection). These ratios were two-fold higher when compared to ^{67}Ga-DOTA, indicating the positive role of metronidazole in increased tumour uptake. PET images with **82** clearly delineated the implanted FM3A tumours, and autoradiography confirmed heterogeneous biodistribution within the tumours [96].

At the same time, Fernández *et al.* independently reported the synthesis and radiolabelling of **84** and the novel triazole-containing ligand 10-[{*N*-methyl-[1-2-(2-methyl-5-nitro-1-*H*-imidazole-1-yl)ethyl-1-*H*-1,2,3-triazole-4-yl]methylaminocarbonylmethyl}]-1,4,7,10-tetrazocyclododecane-1,4,7-triacetic acid (DOTA-TZ-MN) (**86**) [97]. Radiolabelling with ^{68}Ga at pH 4.5 and 95 ^{0}C provided the ^{68}Ga-complexes in high radiochemical purity (>90%). They were stable up to 4 h in aqueous solution and 2 h in human plasma, with no evidence of transchelation of gallium even in the presence of excess diethylene triamine pentaacetic acid (DTPA). ^{68}Ga-DOTA-MN1 (**85**) and **86** were less lipophilic (log*P* -1.65 and -3.30; respectively) than FMISO. *In vitro* and *in vivo* studies were conducted alongside FMISO as the control. The HSF for **85** and **86** in human colon adenocarcinoma HCT-15 cells were 3.3 and 2.1; respectively.

ISSN: 2057-3782 (Online)
http://dx.doi.org/10.17229/jdit.2015-0415-015

Biodistribution profiles obtained from C57 mice, bearing Lewis lung carcinomas, revealed that the compounds provided more favourable T/M ratios and faster soft tissue clearance when compared to FMISO. The T/M and T/B ratios at 2 h post-injection were 5.1 and 1.4 for **85**, 6.6 and 1.2 for **86** and 4.4 and 2.9 for ^{18}F-FMISO.

5.3. Indium nitroimidazole complexes

The radiochemistry of indium parallels that of gallium in terms of half-life (2.8 days) and decay characteristics [98]. Indium-111 decays *via* electron capture (EC) with gamma emissions having 173 keV (89%) and 247 keV (94%) energies, thus, making it a very useful clinical SPECT imaging agent [98-99]. Furthermore, the emission of Auger electrons offers potential for radiotherapeutic applications [100].

Gallium and indium are sister elements, belonging to Group 13 and thus, both have similar chemistries [98]. In aqueous solution, the stable indium cation has a +3 oxidation state (In^{3+}) with a d^{10} electronic configuration. At pH~6, it forms insoluble amphoteric $In(OH)_3$, which dissolves under strong acidic and basic conditions. Indium-111 has a cationic radius of 0.81Å compared to Ga^{3+} (0.62 Å), and it prefers higher coordination numbers [98]. In addition to octahedral complexes, it can also accommodate more donor groups to form 7- and 8-coordinate complexes. Polydentate ligands having carboxylate and amino functionalities are good chelating partners [99].

The bifunctional complexing agents 1,4,8-triazacyclononanetriacetic acid (NOTA) and 1,4,7,10-tetraazacyclododecane-1,4,7-tri-[(methylene)methylphosphonic acid] (DO3PA) were derivatized and labelled with ^{111}In to form ^{111}In-DO3PA-NI (**87**), ^{111}In-NOTA-NI-1 (**88**) and ^{111}In-NOTA-NI-2 (**89**), each having a neutral charge (Figure 33) [81]. Only **88** was examined in mice bearing KHT sarcomas. The lack of selective localization in hypoxic tissue was rationalized to be due to the high molecular weight that may preclude cellular uptake; no further details were presented.

Indium-nitroimidazole complexation has also been used to reduce the rapid clearance of the gastrin-releasing peptide receptor (BB2r)-targeted conjugates. It was postulated that the retention and hence effectiveness of these BB2r complexes could be modulated by exploitation of the hypoxia-trapping capability of the 2-nitroimidazole prodrug. For this purpose, ^{111}In-labelled BB2r conjugates that incorporated up to three 2-nitroimidazole moieties were developed [101-102]. The peptide components were prepared using standard solid-phase peptide synthesis.

The pre-labelling BB2r conjugates 1-4 (Figure 34) were synthesized using the DOTA-**X**-(8-14)NH_2 paradigm. Radiolabelling was carried out by incubation of $^{111}InCl_3$ with each BB2r-DOTA conjugate in ammonium acetate buffer at 90 ^{0}C for 1 h to afford the complexes **90**, **91**, **92** and **93** in 32, 24, 27 and 36% radiolabelling yields, respectively, all with radiochemical purities of >95%. In *in vitro* competitive binding assays using PC-3 cells with [^{125}I-Tyr$_4$]-Bombesin as the competitive radioligand, the binding

ISSN: 2057-3782 (Online)
http://dx.doi.org/10.17229/jdit.2015-0415-015

affinity of the radiolabelled conjugates followed the order **91** > **90** > **92** > **93**. This indicated that the loss of binding affinity in **92** and **93** was primarily caused by steric interference of the 2-nitroimidazole moieties with the BB2r-targeting vector.

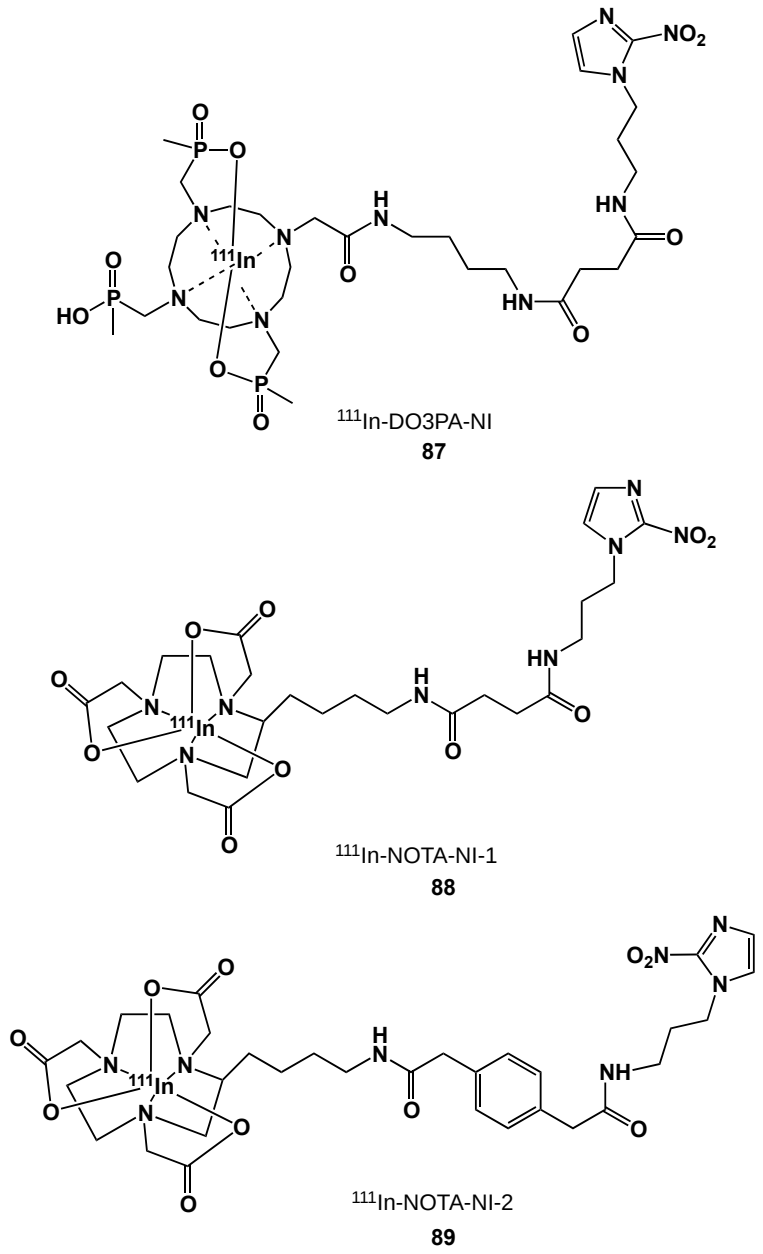

Figure 33. ^{111}In NOTA nitroimidazole complexes (87-89).

ISSN: 2057-3782 (Online)
http://dx.doi.org/10.17229/jdit.2015-0415-015

The effects of the 2-nitroimidazole moieties on the retention of these ^{111}In-labelled conjugates upon 2 h incubations with PC-3 cells under normoxia demonstrated 22% and 20% uptake, respectively, for **90** and **91**, compared to only 1.4 and 0.8% for **92** and **93**. This decline in radioactivity internalization of **92** and **93** was rationalized as being due to their poor receptor binding affinity. Under hypoxic conditions, **90** and **91** exhibited lower uptakes (18% and 15%, respectively), while **92** and **93** (1.3% and 1.4%) were basically unchanged from normoxic values. However, in efflux studies under hypoxic conditions, the radioconjugates exhibited higher retention (i.e., 5-14% of radioactivity cleared) in comparison to efflux under normoxic conditions where 29-55% was cleared. Based on efflux data, the HSF (referred to as HEF by the authors) order was **93** (1.83 ± 0.17) > **91** (1.58 ± 0.15), > **92** (1.27 ± 0.12), > **90** (1.08 ± 0.03).

In order to elucidate whether the BB2r-targeted agents bearing 2-nitroimidazole can conjugate to proteins, cellular protein analyses (PC-3 cells) were performed with **90**, **91** and ^{125}I-Tyr$_4$ (control). Complex **90** and ^{125}I-Tyr$_4$ (control) demonstrated 3.1- 5.6% association with protein under both normoxic and hypoxic conditions, whereas **91** demonstrated similar protein association under normoxia but a 3-fold increase under hypoxic conditions; the latter effect was attributed to bioreductive trapping of the 2-nitroimidazole.

In an attempt to improve the binding of these agents, additional BB2r-targeted radioconjugates with extended linking groups (**94**-**97**; Figure 34) were synthesized [102]. During the 2 h incubation period, all radioconjugates demonstrated similar levels of internalization, ranging from 18-22%. The efflux of **94**-**97** under hypoxia was lower than under normoxic conditions. Furthermore, after 8 h of incubation, the retained internalized radioactivity for **94**, **95**, **96** and **97** under hypoxic conditions were 41%, 61%, 69% and 69%, respectively, compared with only 35%, 35%, 33% and 30% retained under normoxia. At 2 h, all four of these 2-nitroimidazole radioconjugates showed a positive linear relationship between HSF and the number of incorporated 2-nitroimidazole moieties. Cellular protein analysis of the control (**94**) demonstrated minimal hypoxic to normoxic protein association ratios (1.08-1.38), which are likely due to reversible, nonspecific binding. On the other hand, the 2-nitroimidazole-containing BB2r-targeted radioconjugates showed a 2-fold increase (3-fold for **97**) under hypoxic conditions at 4-h and 8-h time points.

Due to the similar efflux and protein association properties of **96** and **97**, only radioconjugates **94**, **95** and **97** were investigated in biodistribution studies in PC-3 tumour-bearing SCID mice. Tumour uptakes of 5.8 ± 2.6, 6.1 ± 3.5 and 2.8 ± 1.2 %ID/g, were observed for **94**, **95** and **97**, respectively at 1 h post-injection. All of the radioconjugates demonstrated rapid blood clearance at 1 h post-injection and major renal/urinary elimination. Significant tumour uptake was observed for **95** and **97** at 72 h post injection, with 6.7% and 21.0% retained from the initial 1 h uptake, compared with only 1.5% remaining for **94**. Micro-SPECT/CT images obtained from PC-3 tumour-bearing SCID mice at 1 h post-injections showed a substantial uptake in the abdominal region, which was consistent with the biodistribution studies.

ISSN: 2057-3782 (Online)
http://dx.doi.org/10.17229/jdit.2015-0415-015

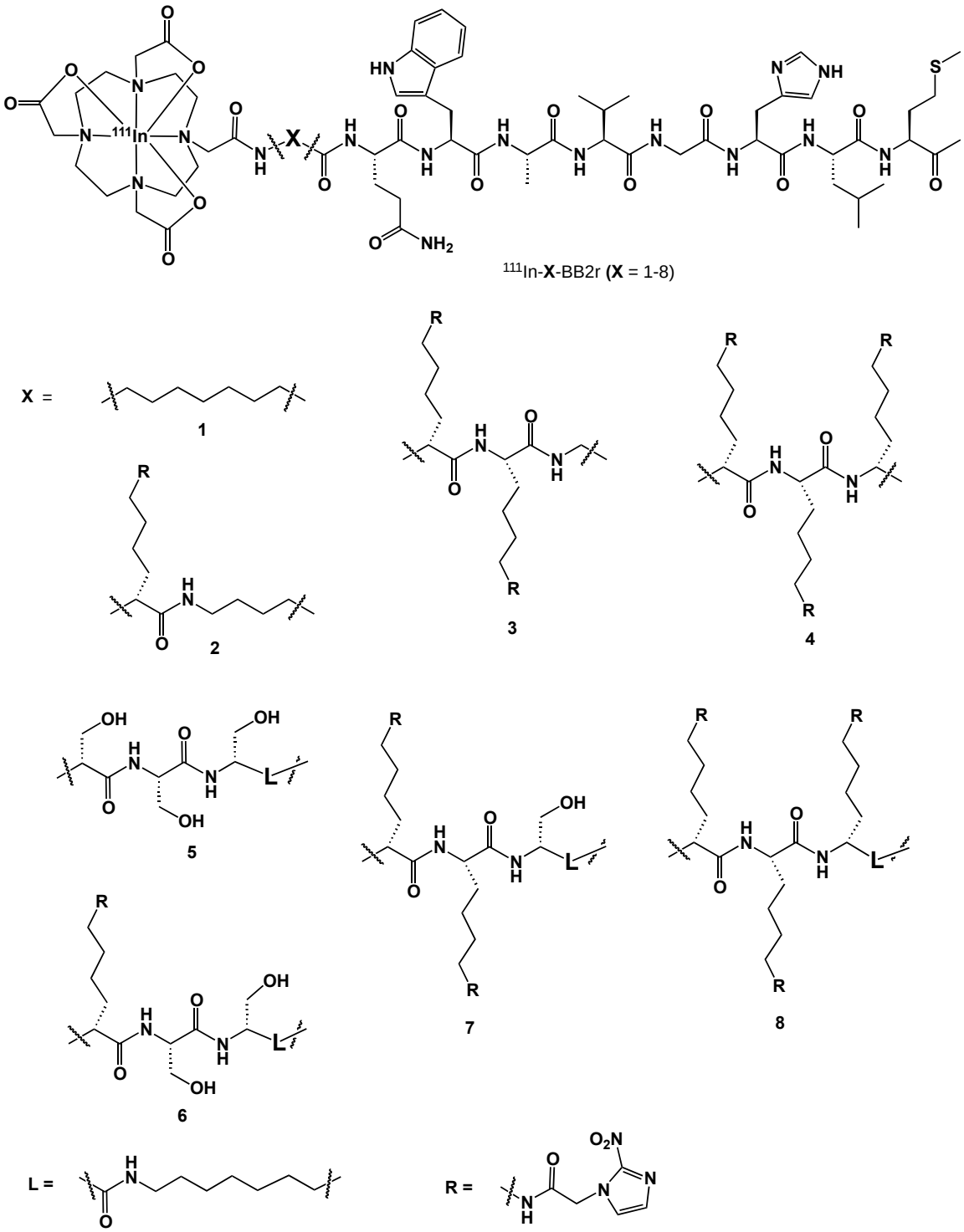

90: ^{111}In-1-BB2r, **91:** ^{111}In-2-BB2r, **92:** ^{111}In-3-BB2r, **93:** ^{111}In-4-BB2r
94: ^{111}In-5-BB2r, **95:** ^{111}In-6-BB2r, **96:** ^{111}In-7-BB2r, **97:** ^{111}In-8-BB2r

Figure 34. ^{111}In-labelled nitroimidazole-BB2r conjugates.

ISSN: 2057-3782 (Online)
http://dx.doi.org/10.17229/jdit.2015-0415-015

Commentary

Several radioisotopes of iodine are useful for imaging (I-123), therapy (I-131) or both (I-124/131), and although radioiodinated compounds are ideal 'matched-pairs' (the same element provides the radionuclides) for imaging and therapy (theranosis) from the chemical perspective, radioiodinated compounds have practical challenges that include labelling processes, radiolabel integrity and decay half-lives. Radiometal coordination compounds extend the concept of 'matched pairs' by enabling the use of different metals for imaging and therapy, having 'masked' them within the electronic structure of the radiometal's ligand. In those cases where the radionuclides of a single element are not suitable for theranostic application, 'matched pairs' comprising of a given bifunctional chelator coordinating radionuclides of two different elements, tethered to the biologically active (targeting) molecule, can deliver unique theranostic performance.

The advantages of bifunctional bioreductive metal complexes containing both a reducible metal core and a bioreductive targeting vector (i.e., nitroimidazole) include possible hypoxia-selective theranosis simply by substituting the metal radionuclide, for example replacing ^{99m}Tc for imaging with ^{186}Re or ^{90}Y for targeted radiotherapy. The complexes with two bioreductive cores in general have also demonstrated potentially greater selectivity for hypoxic tissues than either the metal-complex or the nitroimidazole alone. However replacing the metal functionality may change the coordination chemistry, which may result in quite different pharmacokinetic and biodistribution profiles.

In the case of the nitroimidazole-containing bifunctional radiometal conjugates reviewed in this manuscript, one important caveat to the matched pair concept relates to the metal's intrinsic redox chemistry. Specifically, the transition metals (Cu, Re, Tc) can undergo facile oxygen-sensitive bioreduction to lower oxidation states under mild cellular hypoxia. These reductions occur at higher potentials (i.e., -0.6 V range) compared to the nitroimidazole moiety (> -1 V range) [33], and reduction of the metal core may occur before reduction of nitro group, an effect that may increase sensitivity but decrease selectivity for hypoxic tissue. Not many reports describing bifunctional conjugates containing 2-nitroimidazole and Re or Cu are available, but the roles of these metal cores in hypoxia-selective imaging and the therapy is valid, especially Re-186 and Re-188 which are used in the cancer patients' clinical management.

This redox characteristic does not apply to either the lanthanides or the main group metals because their metal ions are more difficult to reduce. Consequently, lanthanides and main group metals cannot serve as true matched pair metals for transition metal-containing complexes; that is, they cannot be substituted for transition metals when metal-centre bioreduction is a requisite, as is the case for non-nitroimidazole oxygen mimetic radiopharmaceuticals. Papers included in this review provide ample evidence that non-transition metal complexes require nitroimidazole-type components for their hypoxia selectivity, whereas the literature in general is replete with evidence that transition metal complexes can exploit the reductive chemistry of the metal centre itself to achieve hypoxia selectivity. That said, many examples

ISSN: 2057-3782 (Online)
http://dx.doi.org/10.17229/jdit.2015-0415-015

in this review demonstrate that the nitroimidazole moiety contributes to the sensitivity and selectivity of the hypoxia-directed transition (radio)metal core.

The molecular rationale for the development of radiopharmaceuticals derived from nitroimidazoles for molecular imaging and effective therapy of tumours lies in their cellular oxygen-sensitive bioreductive activation. To reiterate, low oxygen tension (hypoxia) leads to the reversible single electron reduction of nitroimidazoles, thereby creating highly reactive radical anions that are reversibly reoxidized to the original compound in the presence of oxygen. Further reduction results in the formation of reactive intermediates that undergo selective trapping and accumulation in hypoxic cells. Clearly, the selectivity of putative bioreductive substrates depends on their reducibility (electron affinity) under cellular redox conditions. The correlations between electron affinity and radiosensitization efficacy are themselves dependent on the method used to derive electron affinity parameters from the experimentally measured reduction voltages.

Such correlations were initially derived from single electron reduction potentials (SERP) as determined by pulse radiolysis (E^1_7 in mV, relative to the hydrogen electrode) [103]. The pulse radiolysis technique is not generally available to most casual users in need of electrochemical measurements and, as a result, reduction potentials are often determined by the hanging-drop mercury polarography and quoted as 'half-wave' ($E^{1/2}$ in mV, relative to the calomel electrode) potentials [104]. More recently, the quasi-reversible reduction potential derived by cyclic voltammetry in a three electrode system of reducing and reoxidizing the substrate has been applied; here, the SERP is defined as E^o in mV, derived as the mean of the anodic and cathodic peak potentials [105].

The relationships of these measured reduction voltages to each other, and more importantly, their correlation to bioreduction and radiosensitizer efficacy have not been established. Furthermore, it has long been known that the correlation between electron affinity and efficacy of a radiosensitizer is subject to modulation by a number of other molecular factors, so that reduction potentials should be used as a no more than a guide to selecting promising hypoxia-selective agents [106-108].

Thus, although Table 1 provides SERPs, or other reduction metrics, cautious interpretation of these summary data are recommended. Similarly, the partition coefficient data (log*P*) (Table 1) have been correlated with efficacy [109]. Although the methodology to measure partition coefficients is relatively standardized, partition data serve only as guides to compound selection rather than as hard determinants.

In general, rapid, high efficiency labelling chemistry that produces a stable, ready-to-inject product, i.e., without further purification, is important for the preparation of radiopharmaceuticals. Availability and cost of radionuclides, radionuclide half-life, cost of post-labelling purification processes and radiological health are important criteria, and metal-based radiopharmaceuticals frequently meet these requirements. In addition, metals offer greater structural diversity, varied reactivity patterns and unique photo- and electrochemical properties. Thus, a wide array of organometallic radiopharmaceuticals based on the

ISSN: 2057-3782 (Online)
http://dx.doi.org/10.17229/jdit.2015-0415-015

concept of bifunctional chelators have been designed, synthesized and evaluated for their utility as hypoxia markers.

That said, many bifunctional chelates have properties that affect their *in vivo* pharmacokinetic performance, which plays a major role in their ultimate clinical acceptance, utility and efficacy. For example, high molecular weight tends to be associated with plasma protein binding and hepatobiliary excretion, ionization may affect trans-membrane passage (cell penetration) and clearance from blood, and high lipophilicity may promote non-specific associations with adipose tissues and membranes.

These properties, where available, are summarized in Table 1, to give the reader an opportunity to compare these properties to biodistribution data.

Table 1. Lipophilicity (Log*P*), reduction potential (V), and tumour/background (T/B) and tumour/muscle (T/M) data in described tumour models for the compounds as reported in the literature

Compound	Log*P*	Reduction Potential (V)	Biodistribution Data		
			Cancer Cell Line	T/B	T/M
1	1.13	-0.58[a]			
2	1.11	-0.57[a]	EMT6	1.08[c]	2.14[c]
3	1.45	-0.63[a]	EMT6	1.17[c]	1.87[c]
4	2.13				
5	-3.0		EMT6, R3327-AT, R3327-H	2.4[d], 1.6[d], 1.2[d]	9[d], 12.3[d], 5.6
6	-2.52		EMT6	5[d]	~50[d]
7	-1.3		R3327-AT	1.5[d]	8.9[d]
8	-0.19		R3327-AT, R3327-H	2.2[d], ~1.5[d]	13.6[d], ~5.0[d]
9	-2.0		EMT6, R3327-AT, R3327-H	6.5[d], 2.1[d], 1.1[d]	12.2[d], 10.9[d], 5.4[d]
19	~1.61	-1.48[b], -1.99[a]	KHT, SCC-VII, RIF-1		3.94[e], 3.34[e], 3.49[e]
20	1.04		KHT-C	0.95[f]	4.37[f]
21			EMT6	2.5[g]	1.0[g]
22	-0.91		KHT	10.32[g]	3.96[g]
23		-1.58[b], -1.31[a]			
24		-1.84[b], -1.30[a]			
25		-1.5[b], -1.29[a]			
26		-1.64[b], -1.34[a]			
27		-1.60[b], -1.32[a]			
28		-1.56[b], -1.22[a]			
29		-1.84[b], -1.23[a]			
30		-1.56[b], -1.83[a]			
31		-1.58[b], -1.83[a]			

ISSN: 2057-3782 (Online)
http://dx.doi.org/10.17229/jdit.2015-0415-015

Compound	Log*P*	Reduction Potential (V)	Biodistribution Data		
			Cancer Cell Line	T/B	T/M
33	-0.20				
34	-0.12				
35			13762 (Mammary tumour)	1.01[g]	5.69[g]
36			R3327-AT, R3327-H	1.9[d], 2.26[d]	15.8[d], 16.3[d]
37			R3327-AT	0.8[d]	3.8[d]
38			R3327-AT R3327-H	1.2[d], 1.87[d]	6.1[d], 8.5[d]
39	-1.40		S180	1.5[f]	8.4[f]
40	0.43		S180 U87, A549	1.88[f], 2.06[h] 1.98[f], 1.25[f]	8.60[f], 8.83[h] 13.11[f], 8.48[f]
41	-0.82		fibrosarcoma	n/a	17[j]
42	0.39		fibrosarcoma	<1[j] 0.49	17[j]
43	0.48		HDM1C1 fibrosarcoma	0.61[j]	2.4[j]
44	0.43		HDM1C1 fibrosarcoma		
45	0.28		fibrosarcoma	1.94[k]	
46	0.17		fibrosarcoma	1.72[k]	
47	0.15		fibrosarcoma	1.26[k]	
48	-0.82				
49	-0.44		Lewis carcinoma	1.86[j]	
50	-1.44		H22	0.84[j]	3.12[f]
51			Breast cancer	0.66[f]	7.14[f]
52			barcl-95	0.82[j]	14.67[j]
53	0.12		S180	0.73[f]	3.23[f]
54	0.28		S180	0.70[f]	2.68[f]
55	0.61		S180	0.77[f]	2.17[f]
56	0.56		S180	0.81[f]	2.83[f]
57	-2.56		S180	3.05[g]	5.27[g]
58	-2.49		S180	1.16[g]	4.24[g]
59	0.77		3LL Lewis murine lung carcinoma	1.0[f]	2.0[f]
60	1.2		n/a	n/a	n/a
61	-1.11		S180		0.61[g]
62	-0.44		S180		0.14[g]
63	-1.64		S180		0.26[g]
64				0.62[j]	3.3[j]
65	-3.05, -2.96				
66	0.45				
71			KHT	0.268[f]	
72			fibrosarcoma	4.3[j]	10.7[j]
75			CT-26	0.49[g]	14.50[c]
76			CT-26	0.50[g]	37.44[g]
78	-2.71			0.6[c]	2.1[c]

ISSN: 2057-3782 (Online)
http://dx.doi.org/10.17229/jdit.2015-0415-015

Compound	Log*P*	Reduction Potential (V)	Biodistribution Data		
			Cancer Cell Line	T/B	T/M
80	-4.60			~0.9[g]	3.96[g]
81	-4.50			~1.5[g]	12.5[g]
83			NFSa FM3A	4.5[e] 7.2[j]	4.4[e] 18[j]
84			FM3A	3.27[j]	9[j]
85	-1.65		Lewis carcinoma	1.4[g]	5.1[g]
86	-3.30		Lewis carcinoma	1.2[g]	6.6[g]

Notes: [a] Redox potential of the radionuclide. [b] Nitroimidazole reduction potential. Highest T/B or T/M ratios were obtained at [c] 1 h, [d] 5-6 h, [e] 6 h, [f] 4 h, [g] 2 h, [h] 5 h, [I] 8 h, [j] 3 h or [k] 30 min post-injection time. (See references for further details).

Acknowledgements

The authors sincerely acknowledge Alberta Innovates Health Solutions (AIHS) for Hypoxia CRIO Program (PK, grant #201201164) and CRIO Project Cancer awards (PK, grant #20131053).

References

Key Article References: 1, 5, 27, 38, 47, 50, 53, 85, 103, 108

[1] Höckel M, Vaupel P. Tumour hypoxia: definitions and current clinical, biologic, and molecular aspects. *J Natl Cancer Inst.* 2001; 93(4): 266-276.
[PubMed Abstract] [Reference Source]

[2] Vaupel P. Hypoxia and aggressive tumour phenotype: implications for therapy and prognosis. *Oncologist*. 2008; 13(Suppl. 3): 21-26.
[Cross Ref] [PubMed Abstract]

[3] Vaupel P. The role of hypoxia-induced factors in tumour progression. *Oncologist*. 2004; 9(Suppl. 5): 10-17.
[Cross Ref] [PubMed Abstract]

[4] Lee NY, Le QT. New developments in radiation therapy for head and neck cancer: intensity-modulated radiation therapy and hypoxia targeting. *Semin Oncol.* 2008; 35(3): 236-250.
[Cross Ref] [PubMed Abstract]

[5] Seidel S, Garvalov BK, Wirta V, et al. A hypoxic niche regulates glioblastoma stem cells through hypoxia inducible factor 2 alpha. *Brain.* 2010; 133 (Pt 4): 983-995.
[PubMed Abstract] [Reference Source]

[6] Brown JM, Wilson WR. Exploiting tumour hypoxia in cancer treatment. *Nat Rev Cancer*. 2004; 4(6): 437-447.
[Cross Ref] [PubMed Abstract]

[7] Minchinton AI, Tannock IF. Drug penetration in solid tumours. *Nat Rev Cancer*. 2006; 6(8): 583-592.
[Cross Ref] [PubMed Abstract]

[8] Bristow RG, Hill RP. Hypoxia, DNA repair and genetic instability. *Nat Rev Cancer*. 2008; 8 (3): 180-192.
[Cross Ref] [PubMed Abstract]

[9] Nakamura S. Structure of azomycin, a new antibiotic. *Pharm Bull.* 1955; 3: 379-383.
[Cross Ref] [PubMed Abstract]

[10] Thin RN. The nitroimidazole family of drugs. *Br J Vener Dis*. 1978; 54 (2): 69-71.
[PubMed Abstract]

[11] Edwards DI. Nitroimidazole drugs - action and resistance mechanisms. I. Mechanism of action. *J Antimicrob Chemother*. 1993; 31 (1): 9-20.
[CrossRef] [PubMed Abstract]

[12] Biaglow JE, Varnes ME, Roizen-Towle L, et al. Biochemistry of reduction of nitro heterocycles. *Biochem Pharmacol.* 1986; 35(1): 77-90.
[CrossRef] [PubMed Abstract]

[13] Gray LH, Conger AD, Ebert M, Hornsey S, Scott OC. The concentration of oxygen dissolved in tissues at the time of irradiation as a factor in radiotherapy. *Br J Radiol.* 1953; 26: 638-648.
[CrossRef] [PubMed Abstract]

[14] Adams GE, Dewey DL. Hydrated electrons and radiobilogical sensitisation. *Biochem Biophys Res Commun*. 1963; 12: 473-477.
[CrossRef] [PubMed Abstract]

[15] Bacchu V, Kumar P, Wiebe LI. The chemistry and radiochemistry of hypoxia-specific radiohalogenated nitroaromatic imaging probes. *Semin Nuc Med.* 2015; 45: 122-135.
[PubMed Abstract]

[16] Hendrickson K, Phillips M, Smith W, Peterson L, Krohn K, Rajendran J. Hypoxia imaging with [F-18] FMISO-PET in head and neck cancer: potential for guiding intensity modulated radiation therapy in overcoming hypoxia-induced treatment resistance. *Radiother Oncol.* 2011; 101(3): 369-375.
[CrossRef] [PubMed Abstract]

[17] Halmos GB, Bruine de Bruin L, Langendijk JA, van der Laan BF, Pruim J, Steenbakkers RJ. Head and neck tumour hypoxia imaging by ^{18}F-fluoroazomycin-arabinoside (^{18}F-FAZA)-PET: a review. *Clin Nucl Med.* 2014; 39(1): 44-48.
[CrossRef] [PubMed Abstract]

[18] Wiebe LI, McEwan AJB. Scintigraphic imaging of focal hypoxic tissue: development and clinical applications of ^{123}I-IAZA. *Braz Arch Biol Technol.* 2002; 45(Spec. Issue): 69-81.
[CrossRef]

[19] Kumar P, McQuarrie SA, Zhou A, McEwan AJB, Wiebe LI. [^{131}I]Iodoazomycin arabinoside for low-dose-rate isotope radiotherapy: radiolabelling, stability, long-term whole-body clearance and radiation dosimetry estimates in mice. *Nucl Med Biol*. 2005; 32(6): 647-653.
[CrossRef] [PubMed Abstract]

[20] Ogawa K, Mukai T. Targeted imaging and therapy for bone metastases: control of pharmacokinetics of bone-targeted radiopharmaceuticals. *J Drug Delivery Sci Technol.* 2009; 19(3): 171-176.
[CrossRef]

[21] Liu S, Edwards DS. Bifunctional chelators for therapeutic lanthanide radiopharmaceuticals. *Bioconjugate Chem.* 2001; 12(1): 7-34.
[CrossRef] [PubMed Abstract]

[22] Ramogida CF, Orvig C. Tumour targeting with radiometals for diagnosis and therapy. *Chem Commun.* 2013; 49(42): 4720-4739.
[CrossRef] [PubMed Abstract]

[23] Tanaka K, Fukase K. PET (positron emission tomography) imaging of biomolecules using metal-DOTA complexes: a new collaborative challenge by chemists, biologists, and physicians for future diagnostics and exploration of in vivo dynamics. *Org Biomol Chem.* 2008; 6(5): 815-828.
[CrossRef] [PubMed Abstract]

[24] Schultz MK, Parameswarappa SG, Pigge FC. Synthesis of a DOTA-Biotin Conjugate for Radionuclide Chelation *via* Cu-Free Click Chemistry. *Org Lett.* 2010; 12(10): 2398-2401.
[CrossRef] [PubMed Abstract]

[25] De Leon-Rodriguez LM, Kovacs Z. The Synthesis and Chelation Chemistry of DOTA-Peptide Conjugates. *Bioconjugate Chem.* 2008; 19(2): 391-402.
[PubMed Abstract]

[26] Bartholomä MD. Recent developments in the design of bifunctional chelators for metal-based radiopharmaceuticals used in Positron Emission Tomography. *Inorg Chim Acta*. 2012; 389, 36-51.
[CrossRef]

[27] Wadas TJ, Wong EH, Weisman GR, Anderson CJ. Coordinating Radiometals of Copper, Gallium, Indium, Yttrium, and Zirconium for PET and SPECT Imaging of Disease. *Chem Rev*. 2010; 110(5): 2858-2902.
[CrossRef] [PubMed Abstract]

[28] Dilworth JR, Parrott SJ. The biomedical chemistry of technetium and rhenium. *Chem Soc Rev*. 1998; 27(1): 43-55.
[Reference Source]

[29] Park J-A, Kim JY. Recent advances in radiopharmaceutical application of matched-pair radiometals. *Curr Top Med Chem.* 2013; 13(4): 458-469.
[CrossRef] [PubMed Abstract]

[30] Price EW, Orvig C. Matching chelators to radiometals for radiopharmaceuticals. *Chem Soc Rev.* 2014; 43(1): 260-290.
[CrossRef] [PubMed Abstract]

[31] Blower PJ. A nuclear chocolate box: the periodic table of nuclear medicine. *Dalton Trans*. 2015; 44(11): 4819-4844.
[CrossRef] [PubMed Abstract]

[32] Archer C, Edwards B, Kelly J, King A, Burke J, Riley A. Technetium labelled agents for imaging tissue hypoxia in vivo. In Technetium and rhenium in chemistry and nuclear medicine, Nicolini, M.; Bandolini, G.; Mazzi, U., Eds. SGE Ditoriali: Padova, Italy, 1995; pp 535-539.
[Reference Source]

[33] Bonnitcha PD, Bayly SR, Theobald MBM, Betts HM, Lewis JS, Dilworth JR. Nitroimidazole conjugates of bis(thiosemicarbazonato)^{64}Cu(II) - Potential combination agents for the PET imaging of hypoxia. *J Inorg Biochem*. 2010; 104(2): 126-135.
[CrossRef] [PubMed Abstract]

[34] Frieden E. Perspectives on copper biochemistry. *Clin Physiol Biochem*. 1986; 4(1): 11-19.
[PubMed Abstract]

[35] Donnelly PS. The role of coordination chemistry in the development of copper and rhenium radiopharmaceuticals. *Dalton Trans.* 2011; 40(5): 999-1010.
[CrossRef] [PubMed Abstract]

[36] Blower PJ, Lewis JS, Zweit J. Copper radionuclides and radiopharmaceuticals in nuclear medicine. *Nucl Med Biol.* 1996; 23(8): 957-980.
[CrossRef] [PubMed Abstract]

[37] Dearling JLJ, Blower PJ. Redox-active metal complexes for imaging hypoxic tissues: structure-activity relationships in copper(II) bis(thiosemicarbazone) complexes. *Chem Commun.* 1998; (22): 2531-2532.
[CrossRef]

ISSN: 2057-3782 (Online)
http://dx.doi.org/10.17229/jdit.2015-0415-015

[38] Paterson BM, Donnelly PS. Copper complexes of bis(thiosemicarbazones): from chemotherapeutics to diagnostic and therapeutic radiopharmaceuticals. *Chem Soc Rev*. 2011; 40(5): 3005-3018.
[CrossRef] [PubMed Abstract]

[39] Bonnitcha PD, Vāvere AL, Lewis JS, Dilworth JR. In Vitro and In Vivo Evaluation of Bifunctional Bisthiosemicarbazone ^{64}Cu-Complexes for the Positron Emission Tomography Imaging of Hypoxia. *J Med Chem*. 2008; 51(10): 2985-2991.
[PubMed Abstract]

[40] Shokeen M, Anderson CJ. Molecular Imaging of Cancer with Copper-64 Radiopharmaceuticals and Positron Emission Tomography (PET). *Acc Chem Res*. 2009; 42(7): 832-841.
[CrossRef] [PubMed Abstract]

[41] Engelhardt EL, Schneider RF, Seeholzer SH, Stobbe CC, Chapman JD. The synthesis and radiolabelling of 2-nitroimidazole derivatives of cyclam and their preclinical evaluation as positive markers of tumour hypoxia. *J Nucl Med*. 2002; 43(6): 837-850.
[PubMed Abstract]

[42] Deutsch E, Libson K, Vanderheyden JL, Ketring AR, Maxon HR. The chemistry of rhenium and technetium as related to the use of isotopes of these elements in therapeutic and diagnostic nuclear medicine. *Int J Rad Appl Instrum B*. 1986; 13(4): 465-477.
[CrossRef] [PubMed Abstract]

[43] Mallia MB, Subramanian S, Mathur A, Sarma HD, Venkatesh M, Banerjee S. On the isolation and evaluation of a novel unsubstituted 5-nitroimidazole derivative as an agent to target tumour hypoxia. *Bioorg Med Chem Lett*. 2008; 18(19): 5233-5237.
[CrossRef] [PubMed Abstract]

[44] Fernandez S, Giglio J, Rey AM, Cerecetto H. Influence of ligand denticity on the properties of novel ^{99m}Tc(I)-carbonyl complexes. Application to the development of radiopharmaceuticals for imaging hypoxic tissue. *Bioorg Med Chem*. 2012; 20(13): 4040-4048.
[CrossRef] [PubMed Abstract]

[45] Mei L, Wang Y, Chu T. ^{99m}Tc/Re complexes bearing bisnitroimidazole or mononitroimidazole as potential bioreductive markers for tumour: Synthesis, physicochemical characterization and biological evaluation. *Eur J Med Chem*. 2012; 58: 50-63.
[CrossRef] [PubMed Abstract]

[46] Giglio J, Fernández S, Pietzsch H-J, et al. Synthesis, in vitro and in vivo characterization of novel ^{99m}Tc-'4+1'-labeled 5-nitroimidazole derivatives as potential agents for imaging hypoxia. *Nucl Med Biol*. 2012; 39(5): 679-686.
[PubMed Abstract]

[47] Mazzi U. The coordination chemistry of technetium in its intermediate oxidation states. *Polyhedron*. 1989; 8(13-14): 1683-1688.
[CrossRef]

[48] Abram U, Alberto R. Technetium and rhenium - coordination chemistry and nuclear medical applications. *J Braz Chem Soc*. 2006; 17(8): 1486-1500.
[CrossRef]

[49] Nunn A, Linder K, Strauss HW. Nitroimidazoles and imaging hypoxia. *Eur J Nucl Med*. 1995; 22(3): 265-280.
[CrossRef] [PubMed Abstract]

[50] Linder KE, Chan YW, Cyr JE, Malley MF, Nowotnik DP, Nunn AD. TcO(PnAO-1-(2-nitroimidazole)) [BMS-181321], a new technetium-containing nitroimidazole complex for imaging hypoxia: synthesis, characterization, and xanthine oxidase-catalyzed reduction. *J Med Chem*. 1994; 37(1): 9-17.
[CrossRef] [PubMed Abstract]

[51] Ballinger JR, Kee JWM, Rauth AM. In vitro and in vivo evaluation of a technetium-99m-labeled 2-nitroimidazole (BMS 181321) as a marker of tumour hypoxia. *J Nucl Med.* 1996; 37(6): 1023-1031.
[PubMed Abstract]

[52] Melo T, Duncan J, Ballinger JR, Rauth AM. BRU59-21, a second-generation ^{99m}Tc-labeled 2-nitroimidazole for imaging hypoxia in tumours. *J Nucl Med*. 2000; 41(1): 169-176.
[PubMed Abstract]

[53] Kumar P, Wiebe LI, Mannan RH, Zhang Z, Xia H, McEwan AJB. [^{99m}Tc]Technetium labelled PnAo-azomycin glucuronides: a novel class of imaging markers of tissue hypoxia. *Appl Radiat Isot.* 2002; 57(5): 719-728.
[CrossRef] [PubMed Abstract]

[54] Hsia C-C, Huang F-L, Hung G-U, Shen L-H, Chen C-L, Wang H-E. The biological characterization of ^{99m}Tc-BnAO-NI as a SPECT probe for imaging hypoxia in a sarcoma-bearing mouse model. *Appl Radiat Isot*. 2011; 69(4): 649-655.
[CrossRef] [PubMed Abstract]

[55] Linder KE, Chan YW, Cyr JE, Nowotnik DP, Eckelman WC, Nunn AD. Synthesis, characterization, and in vitro evaluation of nitroimidazole-BATO complexes: New technetium compounds designed for imaging hypoxic tissue. *Bioconjugate Chem*. 1993; 4(5): 326-333.
[CrossRef] [PubMed Abstract]

[56] Huilgol NG, Chatterjee N, Mehta AR. An overview of the initial experience with AK-2123 as a hypoxic cell sensitizer with radiation in the treatment of advanced head and neck cancers. *Int J Radiat Oncol Biol Phys.* 1996; 34(5): 1121-1124.
[CrossRef] [PubMed Abstract]

[57] Murugesan S, Shetty SJ, Noronha OPD, et al. Technetium-99m-cyclam AK 2123: a novel marker for tumour hypoxia. *Appl Radiat Isot.* 2001; 54(1): 81-88.
[CrossRef] [PubMed Abstract]

[58] Riché F, du Moulinet d'Hardemare A, Sèpe S, Riou L, Fagret D, Vidal M. Nitroimidazoles and hypoxia imaging: synthesis of three technetium-99m complexes bearing a nitroimidazole group: biological results. *Bioorg Med Chem Lett.* 2001; 11(1): 71-74.
[PubMed Abstract]

[59] Ali MS, Kong F-L, Rollo A, et al. Development of ^{99m}Tc-N4-NIM for molecular imaging of tumour hypoxia. *J Biomed Biotechnol*. 2012; 2012: 828139.
[PubMed Abstract]

[60] Nakayama M, Saigo H, Koda A, et al. Hydroxamamide as a chelating moiety for the preparation of technetium-99m radiopharmaceuticals. II. The technetium-99m complexes of hydroxamamide derivatives. *Appl Radiat Isot.* 1994; 45(6): 735-740.
[Reference Source]

[61] Nakayama M, Xu LC, Koga Y, et al. Hydroxamamide as a chelating moiety for the preparation of ^{99m}Tc-radiopharmaceuticals. III. Characterization of various ^{99m}Tc-hydroxamamides. *Appl Radiat Isot.* 1997; 48(5): 571-577.
[CrossRef]

[62] Chu T, Li R, Hu S, Liu X, Wang X. Preparation and biodistribution of technetium-99m-labeled 1-(2-nitroimidazole-1-yl)-propanhydroxyiminoamide (N2IPA) as a tumour hypoxia marker. *Nucl Med Biol*. 2004; 31(2): 199-203.
[CrossRef] [PubMed Abstract]

[63] Chu T, Hu S, Wei B, Wang Y, Liu X, Wang X. Synthesis and biological results of the technetium-99m-labeled 4-nitroimidazole for imaging tumour hypoxia. *Bioorg Med Chem Lett*. 2004; 14(3): 747-749.
[CrossRef] [PubMed Abstract]

[64] Li N, Zhu H, Chu T-W, Yang Z. Preparation and biological evaluation of ^{99m}Tc-N4IPA for single photon emission computerized tomography imaging of hypoxia in mouse tumour. *Eur J Med Chem.* 2013; 69: 223-231.
[CrossRef] [PubMed Abstract]

[65] Mallia MB, Subramanian S, Banerjee S, Sarma HD, Venkatesh M. Evaluation of ^{99m}Tc(CO)$_3$ complex of 2-methyl-5-nitroimidazole as an agent for targeting tumour hypoxia. *Bioorg Med Chem.* 2006; 14(23): 7666-7670.
[CrossRef] [PubMed Abstract]

[66] Mallia MB, Subramanian S, Mathur A, Sarma HD, Venkatesh M, Banerjee, S. Synthesis and evaluation of 2-, 4-, 5-substituted nitroimidazole-iminodiacetic acid-^{99m}Tc(CO)$_3$ complexes to target hypoxic tumours. *J Labelled Compd Radiopharm.* 2010, 53 (8), 535-542.
[CrossRef]

[67] Mallia MB, Subramanian S, Mathur A, Sarma HD, Banerjee S. A study on nitroimidazole-^{99m}Tc(CO)$_3$ complexes as hypoxia marker: some observations towards possible improvement in in vivo efficacy. *Nucl Med Biol.* 2014; 41(7): 600-610.
[CrossRef] [PubMed Abstract]

[68] Wang J, Tian Y, Duan X, et al. Synthesis, radiolabelling and biodistribution studies of [^{99m}Tc(CO)$_3$(MN-TZ-BPA)]$^+$ in tumour-bearing mice. *J Radioanal Nucl Chem*. 2012; 292(1): 177-181.
[CrossRef]

[69] Yang DJ, Ilgan S, Higuchi T, et al. Noninvasive assessment of tumour hypoxia with ^{99m}Tc labeled metronidazole. *Pharm Res.* 1999; 16(5): 743-750.
[PubMed Abstract]

[70] Das T, Banerjee S, Samuel G, et al. ^{99m}Tc-labeling studies of a modified metronidazole and its biodistribution in tumour bearing animal models. *Nucl Med Biol*. 2003; 30(2): 127-134.
[CrossRef] [PubMed Abstract]

[71] Mei L, Sun W, Chu T. Synthesis and biological evaluation of novel ^{99m}TcN-labeled bisnitroimidazole complexes containing monoamine-monoamide dithiol as potential tumour hypoxia markers. *J Radioanal Nucl Chem.* 2014301 (3), 831-838.
[CrossRef]

[72] Wang J, Zheng X, Wu W, Yang W, Yu L. Synthesis and preliminary biological evaluation of ^{99m}Tc(CO)$_3$-labeled pegylated 2-nitroimidazoles. *J Radioanal Nucl Chem.* 2014; 300(3): 1013-1020.
[CrossRef]

[73] Mallia MB, Mathur A, Subramanian S, Banerjee S, Sarma HD, Venkatesh M. A novel [^{99m}TcN]$^{2+}$ complex of metronidazole xanthate as a potential agent for targeting hypoxia. *Bioorg Med Chem Lett.* 2005; 15(14): 3398-3401.
[CrossRef] [PubMed Abstract]

[74] Su Z-F, Zhang X, Ballinger JR, Rauth AM, Pollak A, Thornback JR. Synthesis and Evaluation of Two Technetium-99m-Labeled Peptidic 2-Nitroimidazoles for Imaging Hypoxia. *Bioconjugate Chem*. 1999; 10(5): 897-904.
[CrossRef] [PubMed Abstract]

[75] Zhang Z, Kumar P, Mannan RH, Wiebe LI. ^{99m}Tc-1-[(diphenylphosphino/mercapto)-acetylglycylglycyl-2-aminoethyl]-2-nitroimidazoles as markers of tissue hypoxia. In Technetium, Rhenium and other Metals in Chemistry and Nuclear Medicine, Nicolini, M.; Mazzi, U., Eds. SGE: Padova, 1999; Vol. 5, pp 581-588.
[Reference Source]

[76] Gadolinium: isotope data. Available at: http://www.webelements.com/gadolinium/isotopes.html. Accessed March 21, 2015.

[77] Unterweger MP. Half-life measurements at the National Institute of Standards and Technology. *Appl Radiat Isot*. 2002; 56(1-2): 125-130.
[CrossRef] [PubMed Abstract]

[78] Huang X. Evaluation the decay data of ^{153}Gd. *Appl Radiat Isot.* 2009; 68(1): 18-22.
[Reference Source]

[79] Sherry AD, Caravan P, Lenkinski RE. Primer on gadolinium chemistry. *J Magn Reson Imaging.* 2009; 30(6): 1240-1248.
[CrossRef] [PubMed Abstract]

[80] Rojas-Quijano FA, Tircsó G, Tircsóné Benyó E, et al. Synthesis and Characterization of a Hypoxia-Sensitive MRI Probe. *Chem Eur J*. 2012; 18(31): 9669-9676.
[CrossRef] [PubMed Abstract]

[81] Norman TJ, Smith FC, Parker D, Harrison A, Royle L, Walker CA. Synthesis and biodistribution of ^{111}In, ^{67}Ga and ^{153}Gd-radiolabeled conjugates of nitroimidazoles with bifunctional complexing agents: imaging agents for hypoxic tissue? *Supramol Chem.* 1995; 4(4): 305-308.
[Reference Source]

[82] Pulukkody KP, Norman TJ, Parker D, Royle L, Broan CJ. Synthesis of charged and uncharged complexes of gadolinium and yttrium with cyclic polyazaphosphinic acid ligands for in vivo applications. *J Chem Soc Perkin Trans 2*. 1993; (4): 605-620.
[CrossRef]

[83] Pillai MRA, Chakraborty S, Das T, Venkatesh M, Ramamoorthy N. Production logistics of ^{177}Lu for radionuclide therapy. *Appl Radiat Isot.* 2003; 59(2-3): 109-118.
[CrossRef] [PubMed Abstract]

[84] Das T, Chakraborty S, Banerjee S et al. Preparation and preliminary biological evaluation of a ^{177}Lu labeled sanazole derivative for possible use in targeting tumour hypoxia. *Bioorg Med Chem.* 2004; 12(23): 6077-6084.
[CrossRef] [PubMed Abstract]

[85] Das T, Chakraborty S, Banerjee S, Sarma Haladhar D, Samuel G, Venkatesh M. Preparation and preliminary biological evaluation of a ^{177}Lu labeled nitroimidazole derivative for possible use in targeted tumour therapy. *Radiochim Acta*. 2006; 94: 375-380.
[CrossRef]

[86] Pyun M-S, Hong Y-D, Choi K-H, Lee S-Y, Felipe F, Choi S-J. Preparation and Evaluation of ^{177}Lu Labeled Nitroimidazole Derivative for Targeting Tumour Hypoxia. Transactions of the Korean Nuclear Society Autumn Meeting 2008.
[Reference Source]

[87] Hoigebazar L, Jeong JM, Lee J-Y, et al. Syntheses of 2-Nitroimidazole Derivatives Conjugated with 1,4,7-Triazacyclononane-N,N'-Diacetic Acid Labeled with F-18 Using an Aluminum Complex Method for Hypoxia Imaging. *J Med Chem.* 2012; 55(7): 3155-3162.
[CrossRef] [PubMed Abstract]

[88] Sorger D, Patt M, Kumar P, et al. [^{18}F]Fluoroazomycinarabinofuranoside (^{18}FAZA) and [^{18}F]Fluoromisonidazole (^{18}FMISO): a comparative study of their selective uptake in hypoxic cells and PET imaging in experimental rat tumours. *Nucl Med Biol.* 2003; 30(3): 317-326.
[CrossRef] [PubMed Abstract]

[89] Ritt P, Kuwert T. Quantitative SPECT/CT. *Recent Results Cancer Res*. 2013; 187: 313-330.
[CrossRef] [PubMed Abstract]

[90] Lopci E, Grassi I, Chiti A, et al. PET radiopharmaceuticals for imaging of tumour hypoxia: a review of the evidence. *Am J Nucl Med Mol Imaging*. 2014; 4(4): 365-384.
[PubMed Abstract]

ISSN: 2057-3782 (Online)
http://dx.doi.org/10.17229/jdit.2015-0415-015

[91] Bartholomä MD, Louie AS, Valliant JF, Zubieta J. Technetium and Gallium Derived Radiopharmaceuticals: Comparing and Contrasting the Chemistry of Two Important Radiometals for the Molecular Imaging Era. *Chem Rev.* 2010; 110(5): 2903-2920.
[CrossRef] [PubMed Abstract]

[92] Craig AS, Helps IM, Jankowski KJ, et al. Towards tumour imaging with indium-111 labeled macrocycle-antibody conjugates. *J Chem Soc Chem Commun.* 1989; (12): 794-796.
[Reference Source]

[93] Hoigebazar L, Jeong JM, Choi SY, et al. Synthesis and Characterization of Nitroimidazole Derivatives for ^{68}Ga-Labeling and Testing in Tumour Xenografted Mice. *J Med Chem*. 2010; 53(17): 6378-6385.
[PubMed Abstract]

[94] Hoigebazar L, Jeong JM, Hong MK, et al. Synthesis of ^{68}Ga-labeled DOTA-nitroimidazole derivatives and their feasibilities as hypoxia imaging PET tracers. *Bioorg Med Chem.* 2011; 19 (7): 2176-2181.
[CrossRef] [PubMed Abstract]

[95] Mukai T, Suwada J, Sano K, Okada M, Yamamoto F, Maeda M. Design of Ga–DOTA-based bifunctional radiopharmaceuticals: Two functional moieties can be conjugated to radiogallium–DOTA without reducing the complex stability. *Bioorg Med Chem*. 2009; 17(13): 4285-4289.
[PubMed Abstract]

[96] Sano K, Okada M, Hisada H, et al. In Vivo Evaluation of a Radiogallium-Labeled Bifunctional Radiopharmaceutical, Ga-DOTA-MN2, for Hypoxic Tumour Imaging. *Biol Pharm Bull.* 2013; 36(4): 602-608.
[CrossRef] [PubMed Abstract]

[97] Fernández S, Dematteis S, Giglio J, Cerecetto H, Rey A. Synthesis, in vitro and in vivo characterization of two novel ^{68}Ga-labelled 5-nitroimidazole derivatives as potential agents for imaging hypoxia. *Nucl Med Biol.* 2013; 40(2): 273-279.
[CrossRef] [PubMed Abstract]

[98] Moerlein SM, Welch MJ. The chemistry of gallium and indium as related to radiopharmaceutical production. *Int J Nucl Med Biol.* 1981; 8(4): 277-287.
[CrossRef] [PubMed Abstract]

[99] Boros E, Marquez BV, Ikotun OF, Lapi SE, Ferreira CL. In Coordination chemistry and ligand design in the development of metal based radiopharmaceuticals, John Wiley & Sons Ltd.: 2014; pp 47-79.
[Reference Source]

[100] Fasih A, Fonge H, Cai Z, et al. ^{111}In-Bn-DTPA-nimotuzumab with/without modification with nuclear translocation sequence (NLS) peptides: an Auger electron-emitting radioimmunotherapeutic agent for EGFR-positive and trastuzumab (Herceptin)-resistant breast cancer. *Breast Cancer Res Treat.* 2012; 135(1): 189-200.
[CrossRef] [PubMed Abstract]

[101] Wagh NK, Zhou Z, Ogbomo SM, Shi W, Brusnahan SK, Garrison JC. Development of Hypoxia Enhanced ^{111}In-Labeled Bombesin Conjugates: Design, Synthesis, and In Vitro Evaluation in PC-3 Human Prostate Cancer. *Bioconjugate Chem.* 2012; 23(3): 527-537.
[PubMed Abstract]

[102] Zhou Z, Wagh NK, Ogbomo SM, et al. Synthesis and in vitro and in vivo evaluation of hypoxia-enhanced ^{111}In-bombesin conjugates for prostate cancer imaging. *J Nucl Med.* 2013; 54(9): 1605-1612.
[CrossRef] [PubMed Abstract]

[103] Adams GE, Flockhart IR, Smithen CE, Stratford IJ, Wardman P, Watts ME. Electron-affinic sensitization. VII. A correlation between structures, one-electron reduction potentials, and efficiencies of nitroimidazoles as hypoxic cell radiosensitizers. *Radiat Res.* 1976; 67(1): 9-20.
[CrossRef] [PubMed Abstract]

[104] Olive PL. Correlation between metabolic reduction rates and electron affinity of nitroheterocycles. *Cancer Res.* 1979; 39(11): 4512-4515.
[PubMed Abstract]

[105] Cyclic Voltammetry. Available at:
http://chemwiki.ucdavis.edu/Analytical_Chemistry/Instrumental_Analysis/Cyclic_Voltammetry Accessed March 21, 2015.

[106] Adams GE, Clarke ED, Flockhart IR, et al. Structure-activity relationships in the development of hypoxic cell radiosensitizers. I. Sensitization efficiency. *Int J Radiat Biol Relat Stud Phys Chem Med.* 1979; 35 (2): 133-150.
[CrossRef] [PubMed Abstract]

[107] Adams GE, Clarke ED, Gray P, et al. Structure-activity relationships in the development of hypoxic cell radiosensitizers. II. Cytotoxicity and therapeutic ratio. *Int J Radiat Biol Relat Stud. Phys Chem Med.* 1979; 35(2): 151-160.
[CrossRef] [PubMed Abstract]

[108] Adams GE, Ahmed I, Clarke ED, et al. Structure-activity relationships in the development of hypoxic cell radiosensitizers. III. Effects of basic substituents in nitroimidazole sidechains. *Int J Radiat Biol Relat Stud Phys Chem Med*. 1980; 38(6): 613-626.
[CrossRef] [PubMed Abstract]

[109] Brown JM, Workman P. Partition coefficient as a guide to the development of radiosensitizers which are less toxic than misonidazole. *Radiat Res.* 1980; 82(1): 171-190.
[CrossRef] [PubMed Abstract]

Citation: Ricardo CL, Kumar P, Wiebe LI. Bifunctional Metal - Nitroimidazole Complexes for Hypoxia Theranosis in Cancer. *Journal of Diagnostic Imaging in Therapy*. 2015; 2(1): 103-158.

DOI: http://dx.doi.org/10.17229/jdit.2015-0415-015

Received: 18 March 2015 | **Revised:** 13 April 2015 | **Accepted:** 14 April 2015

Published Online 15 April 2015 http://www.openmedscience.com